Experimental Study on Effect of Reinforcing Steel and Steel Liner on Impact Resistance of RC Panels under Hard Impact

충격 하중을 받은 RC벽체의 내충격 성능에 철근과
강재 라이너가 미치는 영향에
대한 실험적 연구

2023년 2월

서울대학교 대학원
건설환경공학부
예 준 휘

Experimental Study on Effect of Reinforcing Steel and Steel Liner on Impact Resistance of RC Panels under Hard Impact

충격 하중을 받은 RC벽체의
내충격 성능에 철근과 강재 라이너가
미치는 영향에 대한 실험적 연구

지도교수 조 재 열

이 논문을 공학석사 학위논문으로 제출함
2023 년 2 월

서울대학교 대학원
건설환경공학부
예 준 휘

예준휘의 공학석사 학위논문을 인준함
2023 년 2 월

위 원 장 _____ (인)

부위원장 _____ (인)

위   원 _____ (인)

ABSTRACT

Experimental Study on Effect of Reinforcing Steel and Steel Liner under on Impact Resistance of RC Panels under Hard Impact

Ye, Junhwi

Department of Civil & Environmental Engineering

The Graduate School

Seoul National University

The design of nuclear power (NPP) structures is known for its conservative stance to ensure the safety under extreme events such as earthquake, tsunami and even terrorist attacks. Therefore, it requires special design considerations that must be considered in addition to those required in usual civil infrastructures: limitations on yield strength of reinforcing steel, design of containment liner plate (CLP) and impact-resistant design. Especially, limitation on yield strength of rebar has been impeding the efficient design of NPP structure, resulting in high cost of construction and poor concrete quality due to reinforcement congestion. Thus, various research has been conducted to reduce the rebar amount through application of high-strength rebar. In case of CLP, it is installed as an additional layer of containment barrier to prevent radiation leakage. At the same time, CLP is placed as a permanent formwork since the beginning of the construction. Lastly, the United States Nuclear Regulatory Commission has announced an amendment to its regulation since the recent catastrophic accidents, requiring an assessment of large commercial aircraft impact for the construction of newly designed NPPs.

In order to design the NPP structure for its impact resistance against aircraft impact, NPP related design codes such as ACI349-13, DOE-STD-3014-2006 and NEI 07-13 recommended various empirical formulas that were suggested based on impact tests on RC panels. However, the parameters considered in empirical formulas are limited to characteristics of concrete and projectile. In other words, consideration of reinforcement and steel liner, which are the characteristic design factors are not considered in the impact-resistant design of NPP structures. Therefore, it is necessary to investigate the effects of reinforcing steel and steel liner on impact resistance of RC panels to achieve efficient design of NPP structures.

From previous studies on the effects of reinforcement and steel liner on impact resistance of RC panels, it was found that rebar spacing, impact condition and presence of steel liner had significant influence. However, there were few limitations in previous studies which hindered the investigation on the effects of important two components of NPP structures. To specify, most studies did not explicitly study the pure effect of reinforcement owing to different design capacity of test specimens. Moreover, studies on effect of steel liner were conducted without consideration of reinforcing steels, so it was necessary to investigate the relationship between reinforcement and steel liner. Thus, in this study, the research objective was to investigate the effects of rebar spacing, impact condition and presence of steel liner on impact resistance of RC panels under hard impact. Furthermore, based on the experimental results, assessment of existing empirical formulas was conducted, and a modified empirical formula was suggested to reflect the effect of both rebar spacing and steel liner.

A series of impact tests were conducted with yield strength, steel liner, impact velocity, and impact condition as variables. RC panel, steel liner and projectile were designed with geometric similarity ratio to represent the impact of aircraft engine shaft on NPP wall according to specification in NPP design codes. The

impact resistance of RC panels under impact loading was assessed based on perforation resistance and damage assessment of RC panels. To specify, failure mode, residual velocity of projectile and induced surface damages on RC panels were obtained and compared to investigate the effect of each variable in the test program.

Lastly, a modification was made on one of the existing empirical formulas to account for the effect of rebar spacing and the diameter of the projectile. Existing and modified empirical formulas were assessed with test results from this study as well as the previous research. It was found that the modified empirical formula showed the best prediction of perforation limit velocity of RC panels. However, the modification was made based on a single test data from this study, so the reliability of modified empirical formula could be questionable in case with wider range of parameters. Thus, parametric study through numerical simulation of impact test is needed to suggest more robust predictive models for better and reliable evaluation of impact resistance of RC panels in the future.

Keywords: Impact resistance, Aircraft impact test, Steel liner, Empirical formula, High strength reinforcing steel, NPP structures

Student Number: 2021-26749

TABLE OF CONTENTS

LIST OF TABLES

LIST OF FIGURES

NOTATIONS

Symbol		Definition and description
C	=	Ratio of the panel thickness to projectile diameter
DA_{spalling}	=	Normalized damaged area on impacted face
DA_{scabbing}	=	Normalized damaged area on rear face
H	=	Thickness of reinforced concrete panel
M	=	Mass of the projectile
N^*	=	Nose shape factor
P	=	Perimeter of the projectile
V_0	=	Impact velocity of the projectile
V_p	=	Perforation limit velocity
d	=	Diameter of the projectile
f_c	=	Compressive strength of concrete
f_t	=	Tensile strength of the reinforcing steel
f_y	=	Yield strength of the reinforcing steel
h_s	=	Scabbing limit thickness
h_p	=	Perforation limit thickness
u	=	Reference velocity
x	=	Penetration depth
ρ	=	Reinforcement ratio (EWEF)
ρ_c	=	Density of the concrete

1. Introduction

1.1. Research Background

The collapse of nuclear power plant (NPP) structures is considered one of the most hazardous repercussions such as Chernobyl and Fukushima nuclear disasters in 1986 and 2011, respectively. Thus, the design of NPP structures takes a very conservative stance to ensure its safety by requiring three special design considerations: limitation of allowable yield strength of reinforcing steel, design of containment liner plate (CLP) and impact-resistance design.

First of all, the allowable yield strength of reinforcing steel is limited to 420 MPa, causing reinforcement congestion, which is the prominent issue in nuclear industries. This causes poor workability and concrete quality leading to prolonged construction period and structural defects such as honeycomb. Thus, there are numerous on-going research to reduce the amount of reinforcing steel through application of high-strength rebar to NPP structures.

Secondly, containment liner plate in NPP structures is employed as an extra layer of contamination barrier on top of thick concrete wall. At the same time, CLP is placed as a permanent formwork since the beginning of the construction. Consequently, the design of steel liner plate needs to be assessed for its ultimate performance. Thus, there are various research groups investigating its structural performance.

Lastly, the United States Nuclear Regulatory Commission has announced an amendment to its regulation requiring an assessment of large commercial aircraft impact for the new construction of nuclear power plants. Structures under impact load such as aircraft impact may experience local failure such as penetration, scabbing and perforation as shown in Figure 1.1.
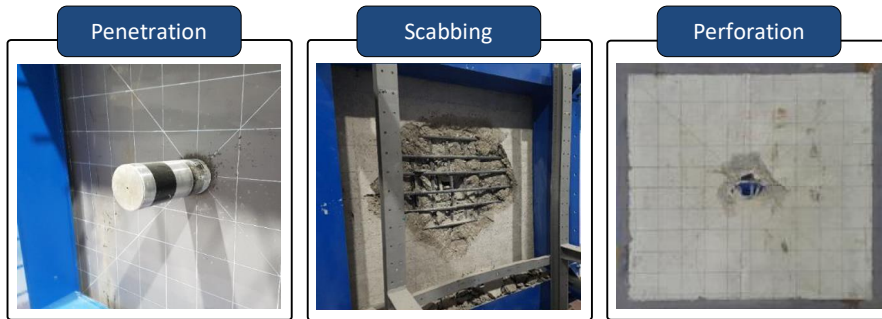
Figure 1.1 Types of local failure under impact loading

Accordingly, each NPP-related design code recommends various empirical formulas listed in Table 1.1 to calculate required wall thickness for preventing local failures under aircraft impact.

Table 1.1 Recommended empirical formulas by NPP design codes

Design codes	Penetration	Scabbing	Designation
ACI 349-13	-	Modified NDRC Bechtel Stone and Webster	Modified NDRC
DOE-STD-3014-2006	Modified NDRC	Modified NDRC Bechtel Chang CRIEPI	Modified NDRC CEA-EDF Degen Chang CRIEPI
NEI 07-13	Modified NDRC	Chang	Degen

1. ACI 349-13: Code requirement for nuclear safety-related concrete structure and commentary

2. DOE-STD-3014-2006: Accident analysis for aircraft crash into hazardous facilities

3. NEI 07-13: Methodology for performing aircraft impact assessment for new plant designs

However, empirical formulas have been proposed without consideration of reinforcing steel and steel liner, which are two crucial elements in the design of NPP structures. For instance, variables are limited to compressive strength and density of concrete, wall thickness, impact velocity, diameter, mass and nose shape of the projectile. Therefore, current empirical formulas may either underestimate or overestimate the impact resistance of RC panels, leading to ineffective and impractical design of NPP structures. Given that, scabbing and perforation modes are considered much more critical since both modes can induce damages to internal equipment and personnel. Accordingly, reviews of empirical formulas for scabbing and perforation limit thickness are followed.

1.1.1. Empirical formulas for scabbing limit thickness

Scabbing limit thickness is defined as minimum required wall thickness to prevent occurrence of scabbing of structures under impact loading. Li et al. (2005) reviewed existing empirical formulas as follows.

1.1.1.1. Modified NDRC formula

This formula was developed based on the ACE formula proposed by U.S. National Defense Research Committee in 1946. All units are in Metric unit.

$$G = 3.8 \times 10^{-5} \frac{N^* M}{d \sqrt{f_c}} \left(\frac{V_0}{d} \right)^{1.8} \tag{1.1}$$

In Eq. (1.1), N^*, M, d, and V_0 denotes the nose shape, mass, diameter and impact velocity of projectile, respectively. And f_c is the compressive strength of concrete. Once G-function is obtained, penetration depth is calculated according to Eq. (1.2a) and (1.2b)

$$\frac{x}{d} = 2G^{0.5} \qquad \text{for } G \geq 1 \tag{1.2a}$$

$$\frac{x}{d} = G + 1 \qquad \text{for } G < 1 \tag{1.2b}$$

In Eq. (1.2a) and (1.2b), x denotes penetration depth of projectile. Scabbing limit thickness h_s can be predicted by following Eq. (1.3a) and (1.3b).

$$\frac{h_s}{d} = 7.91\left(\frac{x}{d}\right) - 5.06\left(\frac{x}{d}\right)^2 \qquad \text{for } \frac{x}{d} \leq 0.65 \text{ or } \frac{h_s}{d} \leq 3 \tag{1.3a}$$

$$\frac{h_s}{d} = 2.12 + 1.36\left(\frac{x}{d}\right) \qquad \text{for } 0.65 \leq \frac{x}{d} \leq 11.75 \text{ or } 3 < \frac{h_s}{d} \leq 18 \tag{1.3b}$$

1.1.1.2. Bechtel formula

Scabbing limit thickness predicted by Bechtel formula is presented as Eq. (1.4) in Metric units. This formula is based on test data applicable to missile impacts on NPP structures under hard projectile.

$$\frac{h_s}{d} = 38.98\left(\frac{M^{0.4} V_0^{0.5}}{f_c^{0.5} d^{1.2}}\right) \tag{1.4}$$

1.1.1.3. Stone and Webster formula

Stone and Webster formula was proposed in non-dimensional form, which can be applied to both Imperial and Metric units.

$$\frac{h_s}{d} = \left(\frac{M V_0^2}{C d^3}\right)^{1/3} \tag{1.5}$$

In Eq. (1.5), there is a dimensional coefficient C that describes the ratio of panel thickness H to diameter of projectile as Eq. (1.6) in Metric units.

$$C = 0.013\left(\frac{H}{d}\right) + 0.330 \tag{1.6}$$

1.1.1.4. Chang formula

Chang suggested a dimensionally homogenous equation for predicting the scabbing limit thickness h_s considering a flat steel cylinder as Eq. (1.7).

$$\frac{h_s}{d} = 1.84 \left(\frac{u}{V_o}\right)^{0.13} \left(\frac{MV_0^2}{d^3 f_c}\right)^{0.4} \tag{1.7}$$

Where, u is the reference velocity of 61 m/s in Metric units.

1.1.1.5. Criepi formula

Criepi suggested a modified version of Chang's formula in Eq. (1.7) by taking different constant for predicting the scabbing limit thickness of RC panel under impact loading as follows.

$$\frac{h_s}{d} = 1.75 \left(\frac{u}{V_o}\right)^{0.13} \left(\frac{MV_0^2}{d^3 f_c}\right)^{0.4} \tag{1.8}$$

1.1.2. Empirical formulas for perforation limit thickness

Perforation limit thickness h_p is defined as minimum required wall thickness to prevent occurrence of perforation of structures under impact loading. Li et al. (2005) reviewed existing empirical formulas as follows.

1.1.2.1. Modified NDRC formula

Modified NDRC predicts the perforation limit thickness with the same formulas for G-function and penetration depth in Eq. (1.1), (1.2a) and (1.2b). It predicts the perforation limit thickness as follows.

$$\frac{h_p}{d} = 3.19 \left(\frac{x}{d}\right) - 0.718 \left(\frac{x}{d}\right)^2 \qquad \text{for } \frac{x}{d} \leq 1.35 \text{ or } \frac{h_p}{d} \leq 3 \tag{1.9a}$$

$$\frac{h_p}{d} = 1.32 + 1.24 \left(\frac{x}{d}\right) \qquad \text{for } 1.35 \leq \frac{x}{d} \leq 13.5 \text{ or } 3 < \frac{h_p}{d} \leq 18 \tag{1.9b}$$

1.1.2.2. CEA-EDF perforation formula

In 1974, original CEA-EDF formula was developed by CEA and EDF in France as follows.

$$\frac{h_p}{d} = 0.82 \frac{M^{0.5} V_0^{0.75}}{\rho_c^{0.125} f_c^{0.375} d^{1.5}}$$ (1.10)

In Eq. (1.10), ρ_c denotes the density of the concrete in Metric units. Li et al. (2005) reviewed ballistic limit velocity, V_p in Metric units, which was further developed by Fullard et al. (1991) to include the rebar ratio term. However, NPP design codes specified CEA-EDF formula as shown in Eq. (1.10).

1.1.2.3. Degen formula

Degen formula was proposed using the penetration depth, Eq. (1.2a) and (1.2b), determined from modified NDRC formula as follows.

$$\frac{h_p}{d} = 2.2\left(\frac{x}{d}\right) - 0.3\left(\frac{x}{d}\right)^2 \qquad \text{for } \frac{x}{d} \leq 1.52 \text{ or } \frac{h_p}{d} \leq 2.65$$ (1.11a)

$$\frac{h_p}{d} = 0.69 + 1.29\left(\frac{x}{d}\right) \qquad \text{for } 1.52 \leq \frac{x}{d} \leq 13.42 \text{ or } 2.65 < \frac{h_p}{d} \leq 18$$ (1.11b)

1.1.2.4. Chang formula

Like scabbing perforation limit thickness, perforation limit thickness uses dimensionally homogeneous equation as follows.

$$\frac{h_p}{d} = \left(\frac{u}{V_0}\right)^{0.25} \left(\frac{MV_0^2}{d^3 f_c}\right)^{0.5}$$ (1.12)

1.1.2.5. Criepi formula

Similar to the equation for scabbing limit thickness in Eq. (1.8), Criepi predicts perforation limit thickness in non-dimensional unit system as follows.

$$\frac{h_p}{d} = 0.90\left(\frac{u}{V_0}\right)^{0.25}\left(\frac{MV_0^2}{d^3 f_c}\right)^{0.5} \qquad (1.13)$$

Thus, to overcome the limitations of existing empirical formulas recommended by NPP design codes, literature review was conducted to investigate the effects of reinforcing steel and steel liner on impact resistance of RC panels in the following section.

1.2. Literature Review

1.2.1. Effect of reinforcing steel on impact resistance of RC panels

Previous studies on effect of reinforcing steel showed that rebar arrangement and impact condition are two main factors that influence the impact resistance of RC panels under impact loading. However, most studies share limitations that the design capacity, ρf_y was not considered as fixed variable, indicating that the impact behavior of RC panel was influenced by both reinforcing steel and its varying design capacity.

1.2.1.1. Huang et al. (2005)

Huang et al. (2005) conducted numerical study on previous impact test (Hanchak et al. (1992)). It was found that the main function of reinforcement comes from the contact between the reinforcing steel and the projectile.
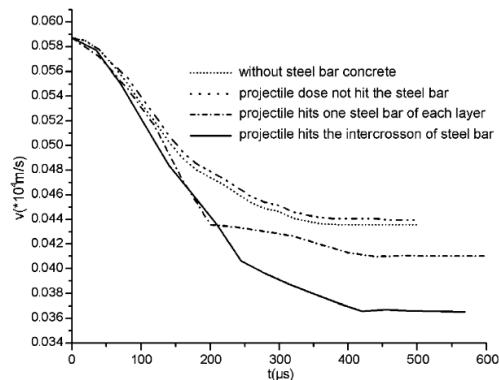
Figure 1.2 Impact velocity history with different condition (Huang et al. (2005))

As shown in Figure 1.2, presence of reinforcing steel in RC panel had little or no influence unless the projectile directly collides the reinforcing steel during the impact. Also, Hanchak et al. (1992) concluded that the effect of striking the reinforcing steel at velocity of 750 m/s had negligible impact on residual velocity projectile. However, the impact velocity of aircraft ranges from 100 – 200 m/s

(Fang et al. (2017)), which is much lower than impact velocities considered in impact tests performed in Hanchak et al. (1992). Therefore, impact tests that could represent the aircraft collision on NPP structures need to be conducted.

1.2.1.2. Dancygier et al. (2007)

Dancygier et al. (2007) performed impact test to investigate the effect of reinforcement ratio on impact resistance of RC panels. Test results were evaluated in terms of perforation resistance and damaged surface area of RC panels. It was found that total amount of reinforcing steel had no effect on perforation resistance, however, damage on rear face showed reduction at relatively high amount of reinforcement volume. Dancygier et al. (2007) also concluded that detailing of reinforcement is important in the design of protective RC panel given that the transverse steel failed during the impact. However, each test specimen with different rebar ratio was designed with the same yield strength, resulting in different design capacity of RC panel. Thus, the effect of reinforcing steel was not explicitly investigated.

1.2.1.3. Abdel-Kader et al. (2014)

Abdel-Kader et al. (2014) investigated the influence of location of reinforcement mesh on perforation resistance of RC panels under hard impact as shown in Figure 1.3.
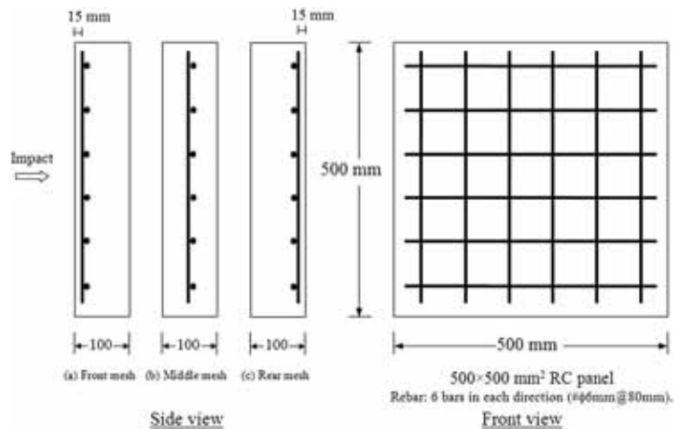
Figure 1.3 Test specimen with different rebar mesh location (Abdel-Kader et al. (2014))

Test results showed that the location of reinforcement mesh, whether placed in the front, middle or rear side of RC panel, had no influence on the impact resistance.

1.2.1.4. Abbas et al. (2021)

Abbas et al. (2021) conducted series of impact tests on RC panels with different rebar spacing and varying rebar diameter to investigate the effect rebar spacing at constant rebar ratio. Total of 4 types of RC panels with 600 by 600 mm panels, with panel thickness of 90mm. As test results, it was found that RC panel with narrower rebar spacing showed better impact resistance. RC panel with narrower rebar spacing showed less ejected concrete although greater crater diameter was observed. Abbas et al. (2021) concluded that the resistance of projectile penetration of punching cone came from the membrane action of reinforcement mesh.

However, the effect of rebar spacing has not been explicitly studied due to different conditions. First of all, the spacing of reinforcement mesh in RC panel with smaller diameter was smaller than the diameter of projectile. Thus, the projectile directly impacted the rebar mesh while RC panel with wider spacing did

not. In other words, the enhancement of impact resistance of RC panel included both effects from narrower spacing and direct resistance of reinforcing steel. Secondly, although rebar ratio was fixed variable in the impact test, the yield strength of rebar used was different in RC panels. Thus, the design capacity of RC panels was changed, impeding the investigation of effect of rebar spacing by itself.

1.2.1.5. Lee et al. (2021)

Lee et al. (2021) performed impact test to investigate the effect of reinforcing steel on impact resistance of RC panels under hard impact. Total of 4 RC panels with varying impact velocity and rebar spacing were conducted with consistent design capacity. It was found that the narrower rebar spacing enhanced the impact resistance of RC panel since the reinforcing steel provided confining and fragment trapping effects. Lee et al. (2021) also conducted numerical study to investigate the effects of yield strength and diameter of reinforcing steel, which showed insignificant influence on impact resistance of RC panels. However, there was only one test specimen where the rebar spacing was changed. Therefore, additional experimental test is needed to investigate impact behavior of RC panels.

1.2.2. Effect of steel liner on impact resistance of RC panels

Previous studies on effect of steel liner on impact resistance showed that steel liner on rear face of RC panel is effective in preventing scabbing and perforation by restraining concrete fragment. As shown in Figure 1.4, presence of steel liner affects the failure mode of RC panel in which the scabbing failure is not observed. However, previous studies did not consider the reinforcing steel as variable, inferring that test results cannot take account for effect of rebar to design the RC panel to prevent local failure under impact loadings.

Figure 1.4 Failure mode in RC with steel liner (Hashimoto et al. (2005))
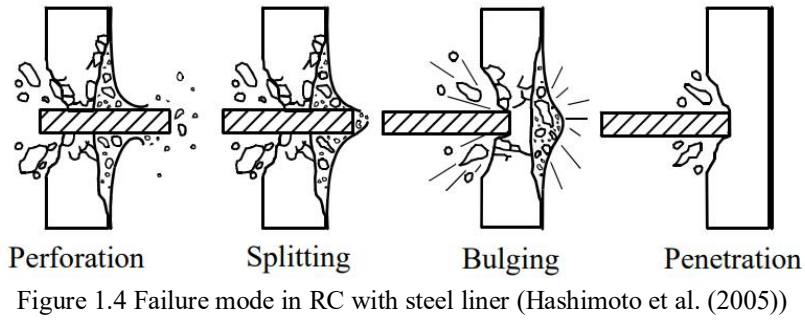
1.2.2.1. Kojima I. (1991)

Kojima conducted series of impact tests on RC panels with and without steel liner to investigate the effect of steel liner on impact resistance of RC panels. Test results showed that the lining the rear face of RC panel with steel plate is effective in prevented scabbing and perforation, however there was no reinforcing effect on concrete panel itself as shown in Figure 1.5.
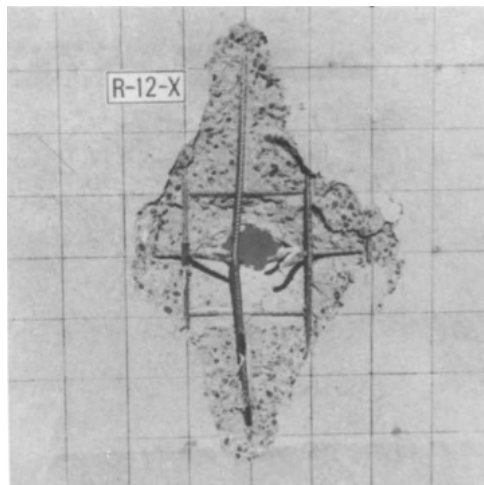
(a) Rear face of RC panel without steel liner
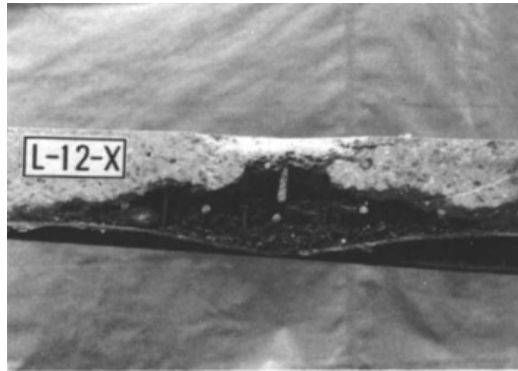
(b) Cross-section of RC panel with steel liner

Figure 1.5 Failure shape of RC panel with and without steel liner (Kojima I. (1991))

However, the rebar spacing was kept constant, and the reinforcement mesh was arranged so that the projectile collided with the rebar. Therefore, test results are incapable of not only isolating the enhancement effect from steel liner but also considering the effect of rebar spacing on impact resistance of RC panel with steel liner.

1.2.2.2. Tsubota et al. (1993)

In this experimental research, the thicknesses of concrete panel and steel liner were main test variables to quantitatively investigate the effect of steel liner under impact loading as shown in Figure 1.6.
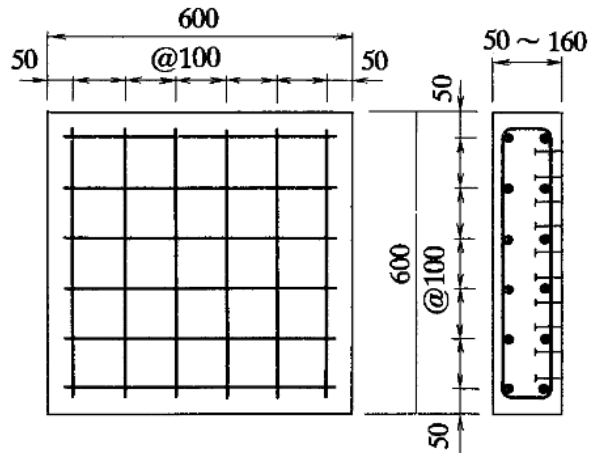
(a) Test panel
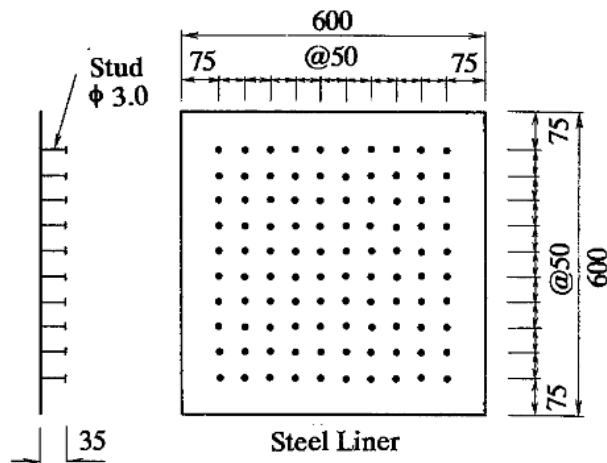
(b) Steel liner

Figure 1.6 Dimensions of test specimens (Tsubota et al. (1993))

The study found that a steel liner attached to the front face showed little effect, while that to the rear face showed remarkable enhancement in preventing scabbing as well as the perforation. The study also proposed an evaluation formula for

1 4

predicting an equivalent concrete thickness for each mode of local failure such as perforation, splitting and bulging. However, the constant rebar spacing of test specimens limited the investigation on effect of reinforcing steel.

1.2.2.3. Hashimoto et al. (2005)

Hashimoto et al. (2005) conducted total of 40 specimen of plain RC, half steel plate RC and steel plate RC to study the effect of steel liner on impact resistance of concrete target as shown in Figure 1.7. And it was found that lining rear face with steel plate is effective in preventing not only the scabbing but also the perforation of projectile as other conclusions from previous research. This study also proposed an evaluation equation for the relationship between the velocity of projectile and bulging height of rear steel plate.
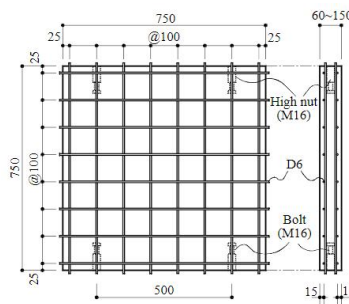
(a) plain RC test specimen
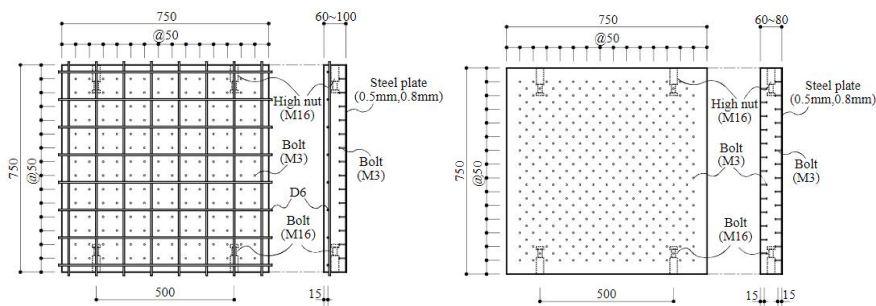
(b) Half steel plate RC   (c) steel plate RC

Figure 1.7. Drawing of test specimens (Hashimoto et al. (2005))

However, the rear reinforcement mesh was removed in half steel RC panel, which was compared to plain RC test specimen with double-layer reinforcement

mesh. Moreover, the proposed equation for RC panel with steel liner employs Chang's formula, which is used to estimate the scabbing limit velocity, but does not consider the effect of reinforcement. Therefore, experimental study is needed to evaluate the impact resistance of steel liner with consideration of effect of reinforcing steel.

1.2.2.4. Galan et al. (2015)

Galan et al. (2015) conducted a series of experimental study to investigate the effects of various slab configurations in comparison with RC panel with only bending reinforcement as base test specimen. To specify, this study focused on the perforation resistance of RC slab with presence of transverse reinforcement, prestressing steels and steel liner. Test results showed that presence of steel liner increased about 20 – 25% in terms of perforation velocity, which means the impact velocity required to initiate perforation failure on the impacted RC panel. However, the tested RC panel included not only the rear side steel liner, but also prestressing steel and T-headed bars for transverse reinforcement. Thus, enhancement effect from steel liner was not explicitly studied in this study.

1.2.2.5. Wu et al. (2015)

In experimental study conducted by Wu et al. (2015), RC panels with varying thicknesses and number of reinforcement layers were loaded with hard projectile impact to investigate the impact resistance. RC panels were reinforced with 1mm-thick steel liners on the rear side and the residual velocity of perforated projectile to evaluate the impact resistance of test specimens. It was found that the effect of steel liner on impact resistance of RC panels was not obvious within the discussed parametric ranges. To specify, the impact velocity considered in this study ranged from 292 to 729 m/s, which is much higher than the expected impact velocity of large commercial aircraft. Therefore, an experimental investigation is needed to

find out about the effect of steel liner at much lower impact velocity range (100 – 200 m/s, Fang et al. (2017))

1.3. Research Objectives and Scope

This study consists of two main objectives. One is the experimental investigation on effects of reinforcing steel and steel liner on impact resistance RC panels under hard projectile impact. To investigate pure effect of each variable, the design capacity of RC panel is kept consistent.

The other objective of the study is to propose a modified empirical formula so that the effects of both rebar and steel liner can be considered in the impact-resistant design of NPP structures.

For these research objectives, a series of scaled impact test to simulate aircraft collision on NPP structures has been conducted. Investigation on effects of rebar spacing, steel liner and rebar collision on impact resistance of RC panel has been conducted through evaluation of perforation resistance and damaged areas on RC panels. With test results, the existing empirical formulas for assessment of local damages on RC panels have been evaluated and a modified empirical formula has been suggested.

2. Experimental Program

In this chapter, the procedure of the impact tests conducted in this study is described including the material test. Material tests were carried out following the standard test method such ASTM C39 and ASTM E8 to obtain concrete compressive strength and tensile strength for reinforcing steel, projectile and steel liner in static state. Impact tests on RC panels are commonly carried out to assess the impact resistance of structures at low-to-mid-velocity impact loading conditions. For the test apparatus, single stage gas gun located at Extreme Performance Testing Center (EPTC) in Seoul National University (SNU). Test variables, method, instrumentations to measure the response are presented in the following sections.

2.1. Material Test

2.1.1. Concrete compressive test

Compressive test for concrete was conducted using MTS 815 equipment at Seoul National University according to ASTM C39. Target concrete compressive strength was 49 MPa, and concrete mix proportion is shown in Table 2.1.

Table 2.1 Concrete mix proportion

Concrete compressive strength (MPa)	Unit weight (kg/m³)				
	Water	Cement	Fine aggregate	Coarse aggregate	Admixture
49	168	577	696	935	5.77

For each test specimen, four of 150×300 mm cylindrical were casted on site and cured in the same conditions as test specimens. Test was carried out with loading rate of 0.5 mm/min (displacement control), and the stress and strain were obtained with installed load cells in testing machine and strain extensometer shown

in Figure 2.1. Test results of concrete specimens are summarized in Table 2.2, and the average compressive strength was 49.8 MPa. Total of 40 cylindrical concrete specimens were casted in two consecutive days, but the average compressive strength for both batches were the same, allowing comparative analysis of the impact test results.

Figure 2.1 Concrete compressive test setup

Table 2.2 Compressive strength of concrete

Specimen ID	f_c (MPa)
SD400-V150-N	48.9
SD400-V200-N	49.3
SD400L-V150-N	51.7
SD400L-V200-N	49.9
SD400-V200-D	49.9
SD600-V150-N	49.7
SD600-V200-N	48.2
SD600L-V150-N	49.8
SD600L-V200-N	51.6
SD600-V200-D	49.7

2.1.2. Reinforcing steel tensile test

Tensile test for reinforcing steel was conducted using 5000kN Universal Testing Machine (UTM) at EPTC according to ASTM E8M. The diameter of reinforcing steel was D25, and SD400 and SD600 rebars were tested at 1mm/min displacement-controlled loading rate. Five specimens were prepared for each type of reinforcing steel and strain data was obtained with video extensometer as shown in Figure 2.2. Test results are described in Table 2.3.
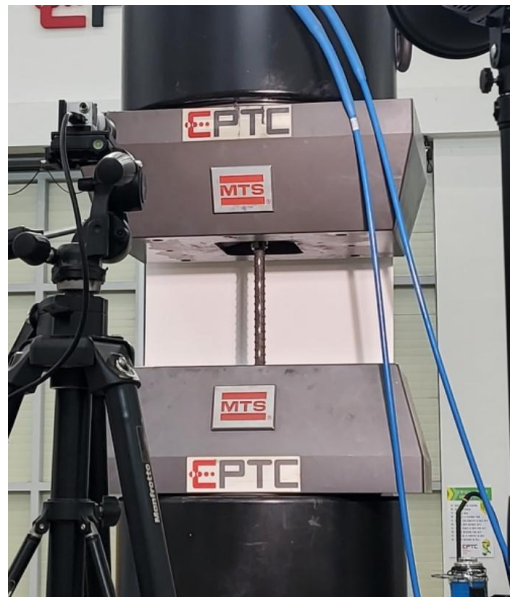
Figure 2.2 Reinforcing steel tensile test setup

Table 2.3 Reinforcing steel tensile test results

Specimen	Nominal diameter (mm)	f_y (MPa)	f_t (MPa)	E (GPa)
D25 SD400	25.4	433	563	197
D25 SD600	25.4	648	764	196

Figure 2.3 shows the stress-strain curves of SD400 and SD600 reinforcing steels. As expected for high-strength reinforcing steel, SD600 rebars, exhibited smaller yield plateau and less ductility compared to SD400 rebars.
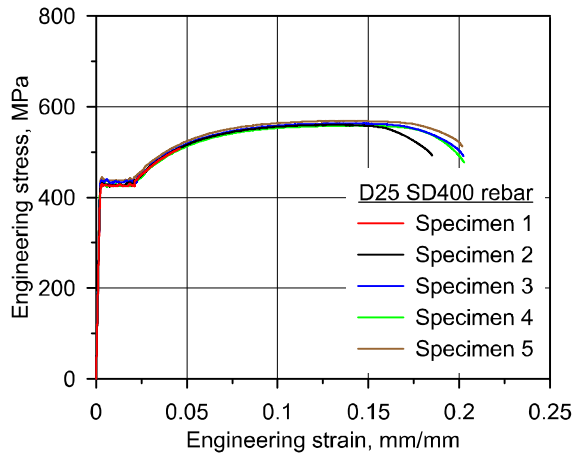
(a) SD400 reinforcing steel
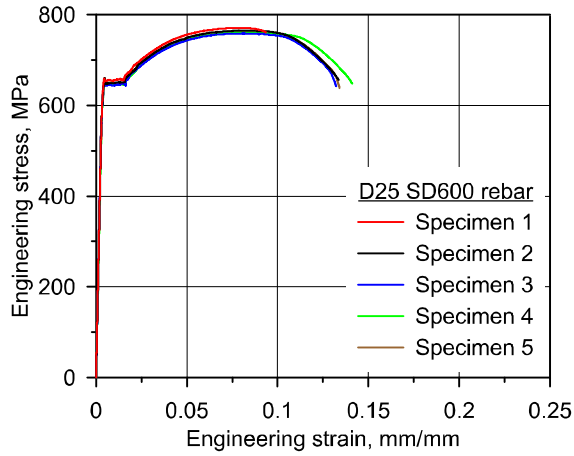
(b) SD600 reinforcing steel

Figure 2.3. Stress-strain curve of reinforcing steel

2.1.3. Steel liner tensile test

Tensile test was carried out with MTS 810 equipment according to ASTM E8M. Three test coupons were prepared as standard rectangular test specimens with nominal width of 12.5mm and nominal thickness of 2.3 mm per ASTM A370-21. Each coupon was marked with 50mm gauge length to obtain strain using the video extensometer as shown in Figure 2.4., and displacement control loading rate of 1mm/min was applied for the test results shown in Table 2.4.

Figure 2.4 Steel liner test setup

Table 2.4 Steel liner tensile test results

Specimen	Width (mm)	Thickness (mm)	f_y (MPa)	f_t (MPa)
1	12.50	2.30	269.2	412.7
2	12.52	2.36	272.2	406.5
3	12.54	2.28	270.7	407.4

The material used for steel liner was SS400, which is the most common structural steel plate used in constructions in Korea. The average yield and ultimate strength were 271 and 409 MPa, respectively.

2.1.4. Projectile tensile test

To obtain material properties of the projectile, three round specimen per ASTM A370-21 were prepared for tensile test using MTS 810 in the test laboratory at Seoul National University. Each specimen was loaded at the rate of 1mm/min according to ASTM E8M, stress data were measured with installed load cells in the machine, and strain was measured with strain gauges and video extensometer as shown in Figure 2.5.

Figure 2.5 Projectile tensile test setup

Table 2.5. and Figure 2.6. show the result of tensile test of the projectile and stress vs. strain curve. The average yield and ultimate strength of the projectile are 450.9 and 531.0 MPa, respectively. The projectile was made of S20C, which is a carbon steel for structural round bar to simulate the hard projectile impact during the test.

Table 2.5 Projectile tensile test results

Specimen	Nominal diameter (mm)	f_y (MPa)	f_t (MPa)
1	12.5	434.4	515.0
2	12.6	471.5	550.5
3	12.6	446.9	527.4
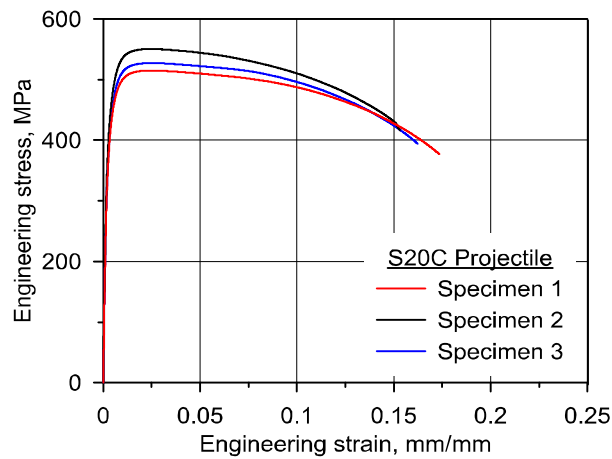
Figure 2.6 Stress-strain curve of projectile

2.2. Impact Test

2.2.1. Introduction

The main objective of impact test was to evaluate the effects of rebar spacing, presence of steel liner and impact condition on impact resistance of RC panel under hard projectile impact. Total of 10 RC panels with 2000 mm width, 2000 mm height, and 500 mm thickness were tested at different impact velocities to obtain responses varying from scabbing to perforation of RC panels. The details of test variables and test specimens are going to be introduced in following sections.

2.2.2. Test Variables

There are three test variables to investigate the effects of reinforcing steel and steel liner on impact resistance of RC panels: rebar spacing, presence of steel liner and rebar collision. In previous study conducted by Lee et al. (2021), the effect of rebar spacing was investigated with application of high-strength rebar at impact velocity of 150 m/s. However, the effect of rebar spacing at higher impact velocity, 200 m/s, was not experimentally studied. Therefore, four test specimens were used to investigate the effect of rebar spacing, and another group of four RC panels with rear steel liner were used for evaluation of impact resistance of steel liner. Lastly, two additional RC panels with intersection at the center of the panel were tested for effects of rebar collision on impact resistance of RC panels. The test variables and designations are shown in table 2.6 and Figure 2.7, respectively. For instance, SD400L-V150-N means that RC panel is reinforced with SD400 rebars and 2.3 mm steel liner, and the projectile impacted between the rebars at impact velocity of 150 m/s. Test plan is shown in table 2.7.

Table 2.6 Test variables and designations

Test variables	Value	Designation
Yield strength of rebar (MPa)	400	SD400
	600	SD600
Steel liner thickness (mm)	0	-
	2.3	L
Impact velocity (m/s)	150	V150
	200	V200
Rebar collision	No rebar collision	N
	Direct collision	D

SD400L - V150 - N

Reinforcing Steel
SD400: f_y = 400 MPa, D25@130mm
SD600: f_y = 600 MPa, D25@180mm

Steel Liner
SD400   none
SD400L   2.3 mm thickness

Impact Velocity
V150   150 m/s
V200   200 m/s

Rebar Collision
N   No rebar collision
D   Direct collision
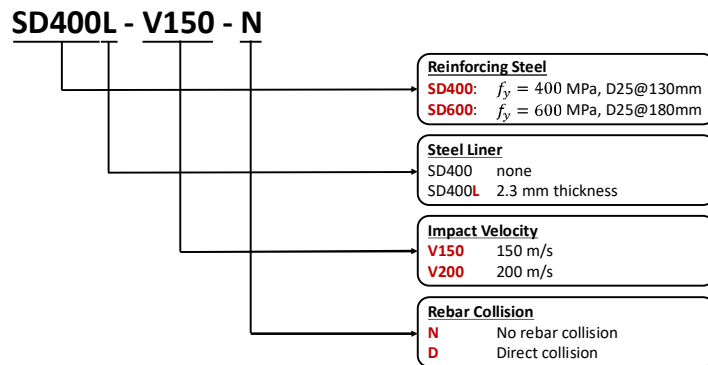
Figure 2.7 Designation for test specimens

Table 2.7 Test plan

Specimen ID	Concrete compressive strength (MPa)	Reinforcement		Projectile		Remark
		Rebar spacing (mm) / Rebar ratio (%)	Steel liner thickness (mm)	Impact velocity (m/s)	Impact condition	
SD400-V150-N	49	130 / 0.87	0	150	No rebar collision	Effect of rebar spacing
SD400-V200-N				200		
SD600-V150-N		180 / 0.63		150		
SD600-V200-N				200		
SD400L-V150-N		130 / 0.87	2.3	150		Effect of steel liner
SD400L-V200-N				200		
SD600L-V150-N		180 / 0.63		150		
SD600L-V200-N				200		
SD400-V200-D		130 / 0.87	0	200	Direct collision	Effect of rebar collision
SD600-V200-D		180 / 0.63		200		

2.2.3. Test specimen

2.2.3.1. Design of RC panels

For the design of RC panels, Shin-Kori NPP 3 (APR1400) was scaled to the similarity ratio of 1:2.4 with respect to the wall thickness since the maximum thickness panel for test equipment is 0.5 m. Table 2.8 shows the detailed material and dimensional properties of NPP structure and scaled panel.

Table 2.8 Design of RC panels

Properties	NPP structure	Test specimen	
	Shin-Kori NPP 3	SD400	SD600
Concrete strength (MPa)	42	49	
Rebar yield strength (MPa)	400	400	600
Rebar diameter	D57	D25	
Panel thickness (m)	1.2	0.5	
Rebar spacing (mm)	305	130	180
Rebar ratio (%)	0.92	0.87	0.63
ρf_y (MPa)	3.68	3.49	3.78

To investigate the effect of rebar spacing, high strength reinforcing steel was placed at wider spacing, so that ρf_y of each panel showed similar values for both actual and scaled cases for maintaining the design capacity of RC panel. For the design of RC panel with direct rebar collision, the reinforcement mesh was arranged so that the intersection of horizontal and vertical rebars is located at the center of the panel as shown in Figure 2.8.
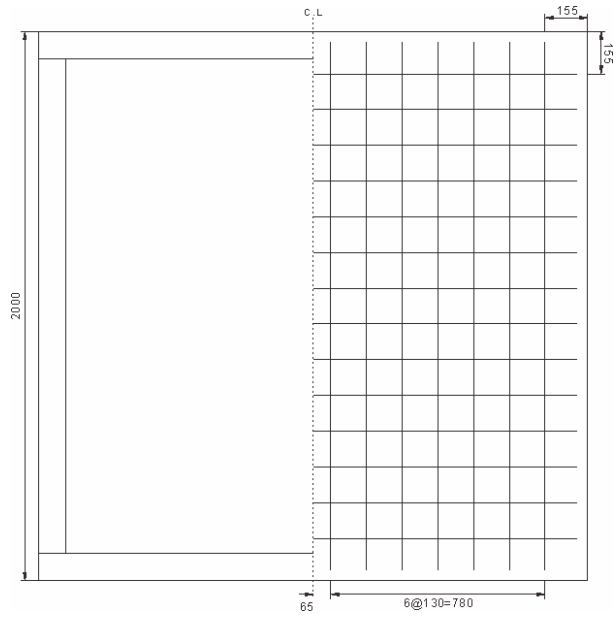
(a) No rebar collision
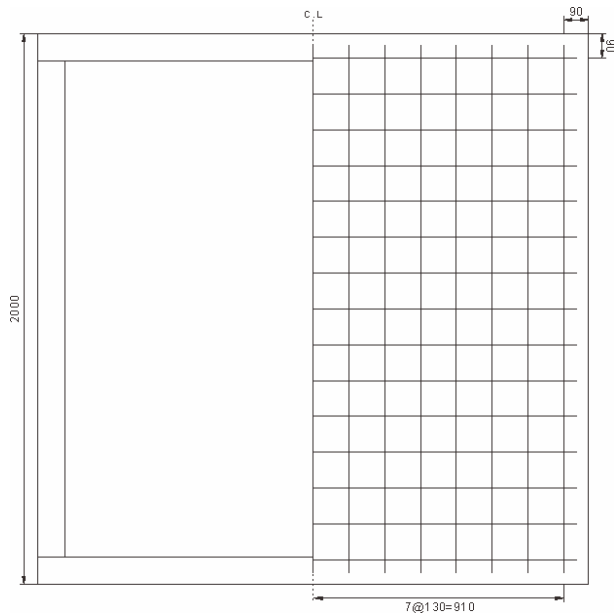
(b) Direct rebar collision
Figure 2.8 Detail of specimens (SD400 panels)

After the assembly of reinforcements, concrete was poured in the mold and cured as shown in Figure 2.9.

(a) assembly of reinforcement

(b) assembly with mold
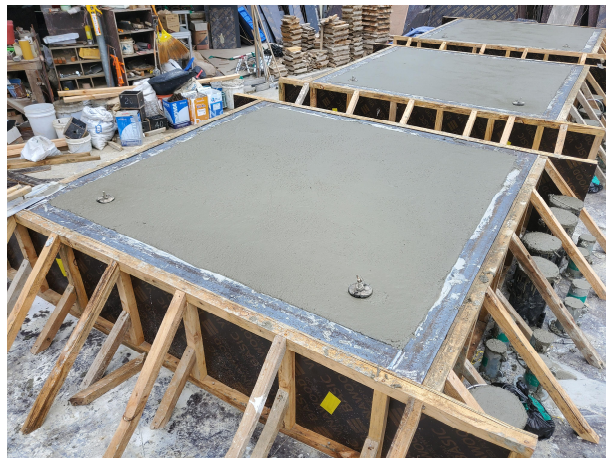
(c) concrete pouring and curing
Figure 2.9 Test specimen fabrication

2.2.3.2. Design of steel liner

For the design of steel liner, the drawing of CLP used in Shin-Kori 5 and 6 was used as reference. Since the maximum width of available product was 1.5 m, additional strips of steel liner welded on the top and bottom ends. For composite action between concrete panel and steel liner, evenly spaced angle stiffeners were welded to the steel liner as shown in Figure 2.10. Finally, steel liner was attached to the rear side of reinforcement assembly before pouring the concrete.

(a) steel liner with angle stiffener
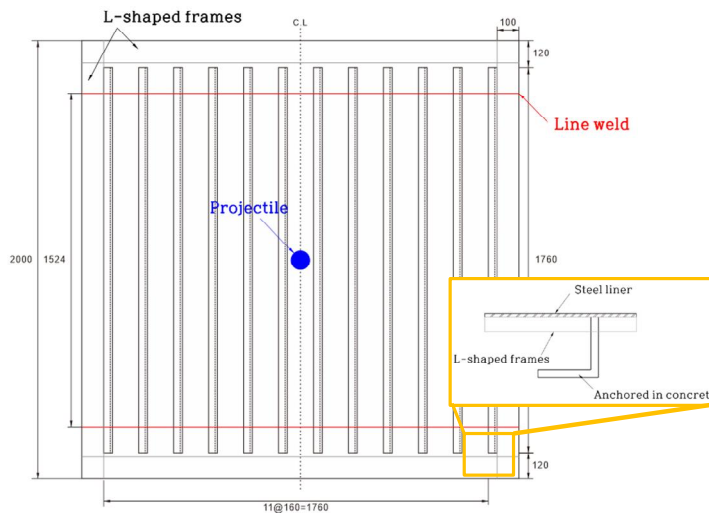
(b) drawing of steel liner

Figure 2.10 Detail of the steel liner

2.2.3.3. Design of projectile

In the assessment of aircraft collision on nuclear facilities, DOE-STD-3014-2006 design code recommended the shaft of aircraft engine as the hard projectile. Thus, turbo fan engine of Boeing 757 was selected as projectile as shown in Figure 2.11.

(a) Drawing of scaled projectile

(b) Hard projectile
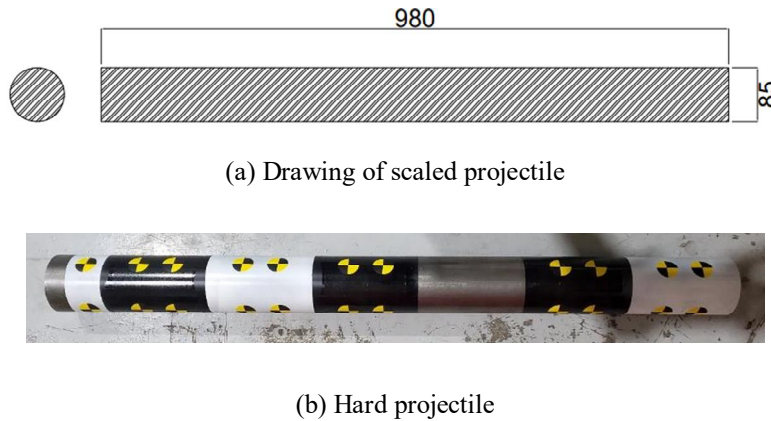
Figure 2.11 Detail of projectile

2.2.4. Test Procedure

All impact tests were conducted with single stage gas gun machine of EPTC at SNU. This particular testing machine can accelerate a 100-kg object up to 470 m/s. The single stage gas gun machine is shown in Figure 2.12.
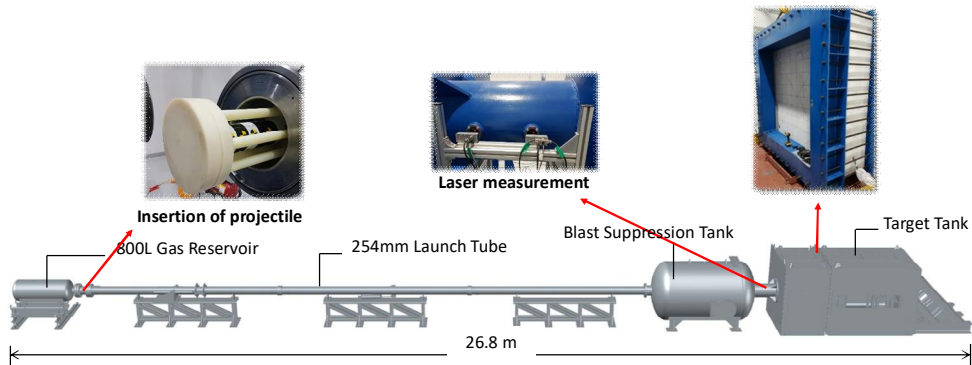
Figure 2.12 Overview of single stage gas gun machine in EPTC at SNU

Projectile is inserted at the left end of the gas gun machine with a body sabot that is designed to ensure straightness of the projectile. When the compressed air is released from 800L gas reservoir, the projectile travels along the 254mm launch tube to reach the blast suppression tank. Then, the sabot is stripped off by the sabot located at the right end of the suppression tank, leaving only projectile to impact the test specimen, which is fixed at both sides by four steel rods in the target tank.

2.2.5. Instrumentations

2.2.5.1. Strain gauges at supports

As mentioned before, aircraft collisions are expected to cause structures to experience local failure such as penetration, scabbing and perforation. In other words, impact loading induces failure of structural component without collapse of the whole structure. Consequently, structures under impact loadings inherently show less reaction forces at the support since most of the impact force dissipates from the formation of local failures.

In this study, reaction forces in the rods that are supporting the target frame are obtained by attaching four strain gauges as shown in Figure 2.13. Since support rods are designed to behave elastically at its maximum capacity, obtained strain is multiplied by the modulus of elasticity to get the stress experienced by the rod. Finally, the reaction force can be obtained by multiplying the average stress of each rod.
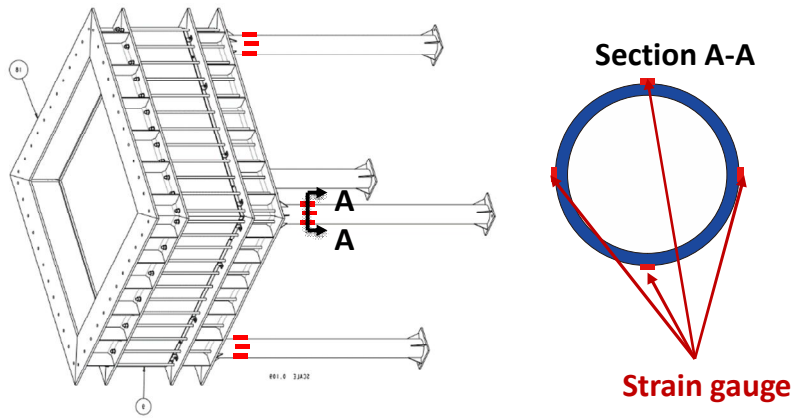
(a) Strain gauges at the supporting rod
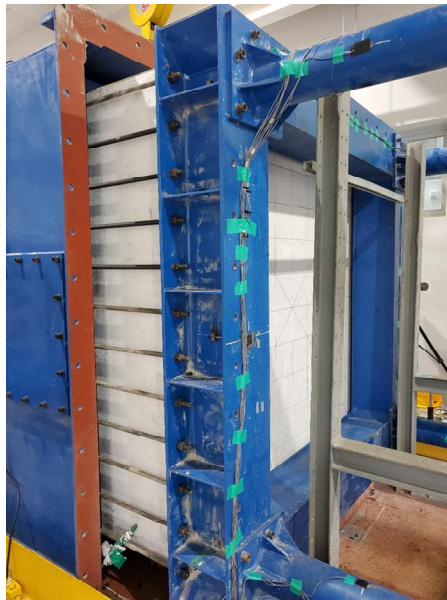
(b) strain gauges on the rear side of target tank
Figure 2.13 Strain gauges for reaction forces

2.1.5.2. High Speed Camera and Data Acquisition

To assess the impact resistance of RC panel under impact loading, two high-speed cameras were used in this study. One is to capture the behavior of RC panel on the impacted side and to measure the impact velocity of the projectile. Another is placed at the rear side of the panel to measure the residual velocity of the perforated projectiles. Test setup for high-speed cameras is shown in Figure 2.14.
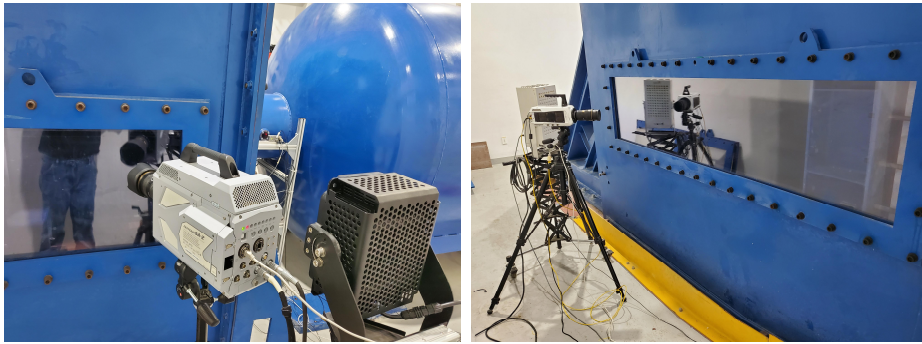
Figure 2.14 High-speed camera setup

In this study, real time processing software developed by DEWETRON was used for data acquisition with sampling rate of 1 MHz, The details of the system are summarized in Table 2.9. Cut-off frequency of strain gauges is determined by comparing raw data with filtered data through low pass filter.

Table 2.9 Details of the data acquisition system

Model	Description	Image
DEWE 800	Control of instrumentation system	
DEWE-50-PCI-32	Channel expansion frame 32 signal converters	
DEWE 30-16	Channel expansion frame 16 signal converters	
HIS-STG-D	Signal converter (General sensor)	
MSI-BR-ACC	Signal converter (Piezoelectric sensor) Signal conversion	
DEWE-ORION-1616-100	A/D converter Conversion of digital signal	

3. Experimental Results

In this study, the evaluation of impact resistance of RC panel was performed with two different categories: perforation resistance and damage assessment of RC panel. Firstly, perforation resistance is discussed in terms of failure mode, residual velocity of projectile and reaction forces at the supporting rods. Damage assessment is conducted by comparing the damaged areas incurred at the front and rear side of the panel, which are called spalling and scabbing areas, respectively. The test results are summarized in Table 3.1.

The impact behavior of RC panel is commonly discussed as the failure mode experienced by the panel after the test. Thus, NPP design codes regulate wall thickness to prevent each type of local failure according to the expected force exerted by the impact. Residual velocity of projectile that fully penetrated the RC panel, could be used to indicate how much portion of the kinetic energy is absorbed or resisted by the RC panel. Thus, effects of rebar spacing, steel liner and rebar collision will be discussed in terms of perforation resistance in the following sections.

For damaged areas on both side of RC panels, namely spalling and scabbing area, are normalized with respect to the total surface area of the RC panels as shown in Eq. (3.1a) and (3.1b). Impact test of SD400-V150-N case was performed with test specimen from previous experiment conducted by Lee et al. (2021).

$$DA_{spalling}\left(\%\right) = \frac{\text{Spalling Area} \left(m^2\right)}{\text{Total Surface Area} \left(m^2\right)} \qquad \text{Eq. (3.1a)}$$

$$DA_{scabbing}\left(\%\right) = \frac{\text{Scabbing Area} \left(m^2\right)}{\text{Total Surface Area} \left(m^2\right)} \qquad \text{Eq. (3.1b)}$$

Table 3.1 Test results

Specimen ID	Dimension [H × B × t] (m)	Impact velocity (m/s)	Residual velocity (m/s)	Failure mode	Damaged areas	
					$DA_{spalling}$ (%)	$DA_{scabbing}$ (%)
SD400-V150-N	2.1 × 2.1 × 0.5	151.4	Rebound	Scabbing	8.56	34.69
SD400-V200-N		203.3	71.4	Perforation	8.00	33.25
SD600-V150-N		151.8	Rebound	Perforation	4.52	39.69
SD600-V200-N		199.8	83.3	Perforation	7.24	41.39
SD400L-V150-N		153.3	Rebound	Bulging	9.06	0.00
SD400L-V200-N	2.0 × 2.0 × 0.5	200.0	52.9	Perforation	8.75	0.00
SD600L-V150-N		151.1	Rebound	Bulging	3.91	0.00
SD600L-V200-N		199.0	48.7	Perforation	10.55	0.00
SD400-V200-D		198.3	Rebound	Perforation	6.05	48.25
SD600-V200-D		200.9	Not measured	Perforation	9.49	47.25

3.1. Perforation resistance

3.1.1. Effect of rebar spacing

At impact velocity of 150 m/s, failure mode experienced by SD400-V150-N and SD600-V150-N panel were scabbing and perforation, respectively. As shown in Figure 3.1, RC panel with wider rebar spacing experienced worse failure mode as the rebar spacing increased from 130mm to 180mm. Although the projectile rebounded after the impact, SD600-V150-N panel just completely perforated. At impact velocity of 200 m/s, both RC panels experienced perforation, and projectile exhibited residual velocity after the perforation. Test results are summarized in Table 3.2.

Residual velocity of projectile showed about 17% increase due to wider rebar spacing, showing decreased resistance against perforation. According to Lee et al. (2021), wider rebar spacing showed inferior impact resistance due to reduced confining effect from reinforcing steels and fragment trapping effect resulted in reduced impact resistance of RC panels. As rebar spacing increased, more concrete fragment was ejected through the wider spacing between rebars. This trend is clearly shown in ejected mass concrete of each RC panel as in Figure 3.2. For SD400 panels that had narrower rebar spacing, about 3.4 – 4.3% of total weight was lost during the impact, but 5.4% of total weight of concrete was lost for SD600 panels at the same impact conditions.
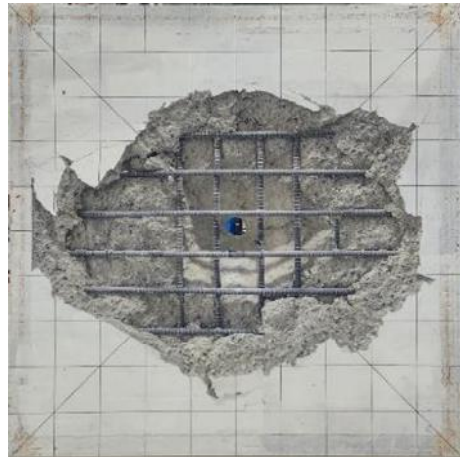
<table>
<tr><td>(a) SD400-V150-N</td><td>(b)SD600-V150-N</td></tr>
</table>
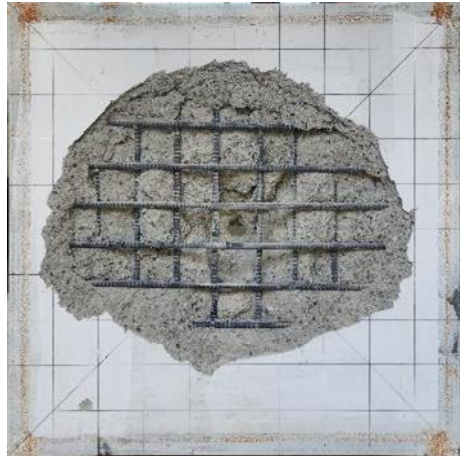
<table>
<tr><td>(a) SD400-V200-N</td><td>(b)SD600-V200-N</td></tr>
</table>

Figure 3.1 Failure shape on rear side of RC panels

Table 3.2 Failure mode and residual velocity

Specimen ID	Failure mode	Residual velocity (m/s)
SD400-V150-N	Scabbing	Rebound
SD600-V150-N	Perforation	Rebound
SD400-V200-N	Perforation	71.4
SD600-V200-N	Perforation	83.3
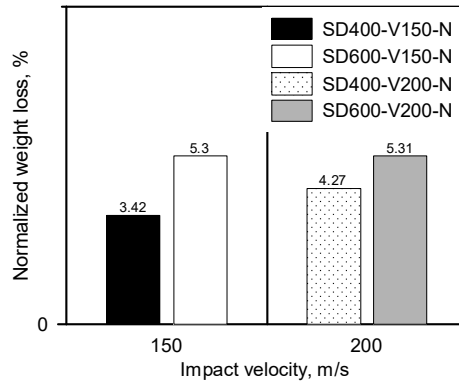
Figure 3.2 Ejected concrete mass of RC panels

According to yield line theory by Goli et al. (1980), the expected reaction force in SD400-V150-N is about 4200 kN. However, the reaction forces measured during the impact test ranged from 336.3 kN to 549.9 kN as shown in Figure 3.3 and Table 3.3. This indicates that most of the applied forces from the projectile was dissipated by the local damages.

(a) SD400-V150-N

(b) SD600-V150-N

(c) SD400-V200-N
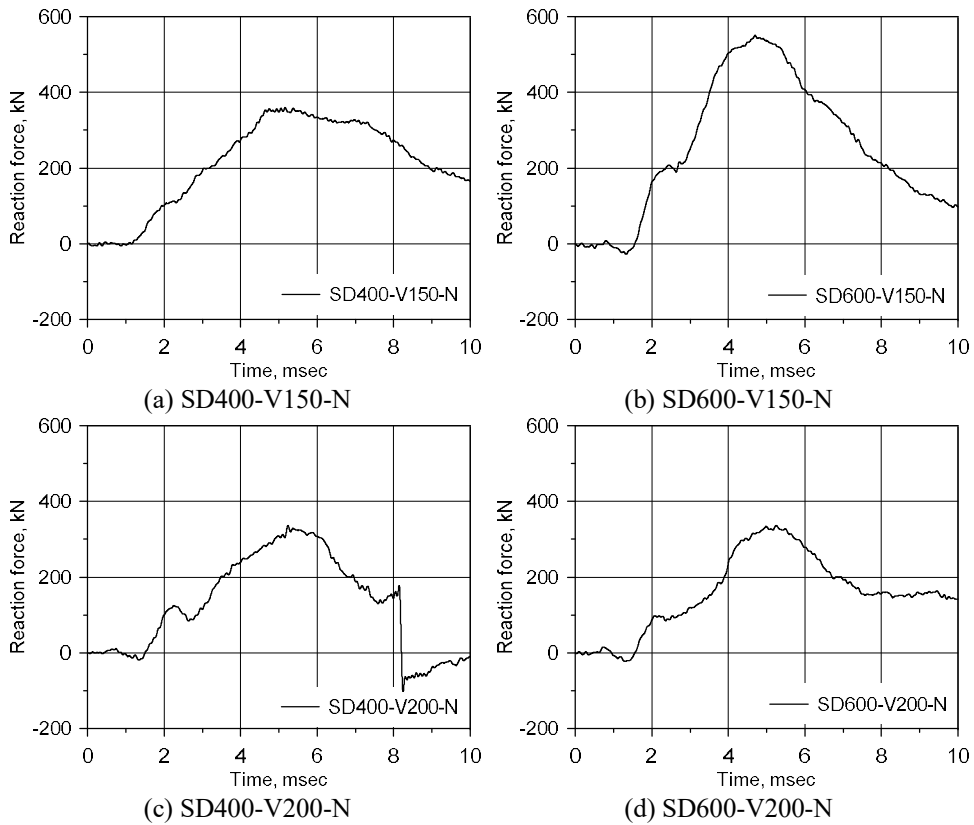
(d) SD600-V200-N

Figure 3.3 Reaction force time history of plain RC panels

Table 3.3 Reaction forces of RC panels

Specimen ID	Reaction force (kN)
SD400-V150-N	359.6
SD600-V150-N	549.9
SD400-V200-N	336.3
SD600-V200-N	336.7

3.1.2. Effect of steel liner

The impact behavior of RC panel with steel liner showed increased resistance against both scabbing and perforation. As mentioned in previous studies (Kojima I. (1991), Tsubota et al. (1993), Hashimoto et al. (2005)), rear steel liner showed great enhancement against scabbing and perforation as both were prevented as shown this study in Figure 3.4. To specify, concrete fragment on the rear side of SD400L-V150-N and SD600L-V150-N was restrained by the steel liner, showing a different failure mode called bulging. This indicates that the steel liner deformed without experiencing major failure, maintaining its role as a radiation barrier in NPP structures.
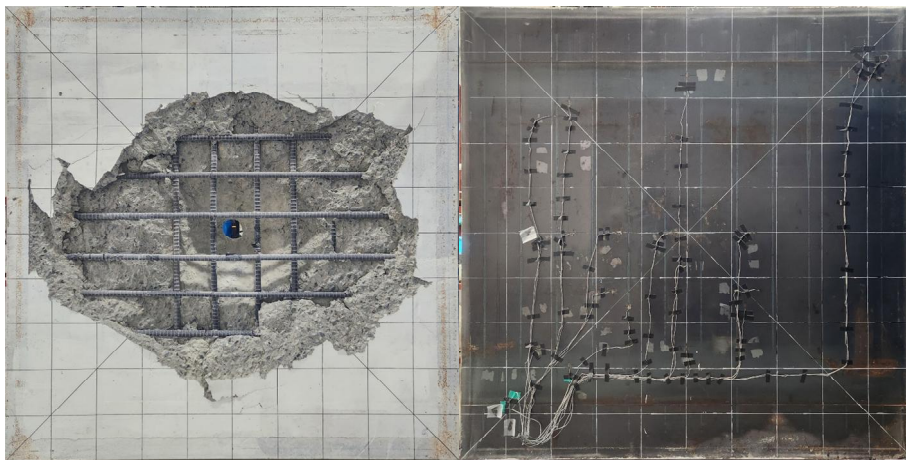
(a) SD600-V150-N   (b)SD600L-V150-N
Figure 3.4 Failure shape at the rear side of RC panels with steel liner

For test cases with impact velocity of 200 m/s, remarkable enhancement in perforation resistance was shown in terms of residual velocity of projectile. Test results for RC panels with steel liner are summarized in Table 3.4.

Table 3.4 Failure mode and residual velocity of RC panel with steel liner

Specimen ID	Failure mode	Residual velocity (m/s)	Reaction force (kN)
SD400L-V150-N	Bulging	Rebound	359.6
SD600L-V150-N	Bulging	Rebound	549.9
SD400L-V200-N	Perforation	52.9	336.3
SD600L-V200-N	Perforation	48.7	336.7

When RC panel is reinforced with a steel liner, the residual velocity of projectile was reduced about 26 – 42% compared to that of plain RC panel. As aforementioned, the steel liner on rear side restrained concrete fragment, acting as another very dense layer of reinforcement mesh resisting the perforation of the projectile. Moreover, the residual velocities measured in both RC panels with steel liners infer that the presence of steel liner reduce the effect of rebar spacing. In other words, reduction in resistance due to the wider rebar spacing was ameliorated by the steel liner as shown in Figure 3.5. And Figure 3.6 shows the reaction forces time history.
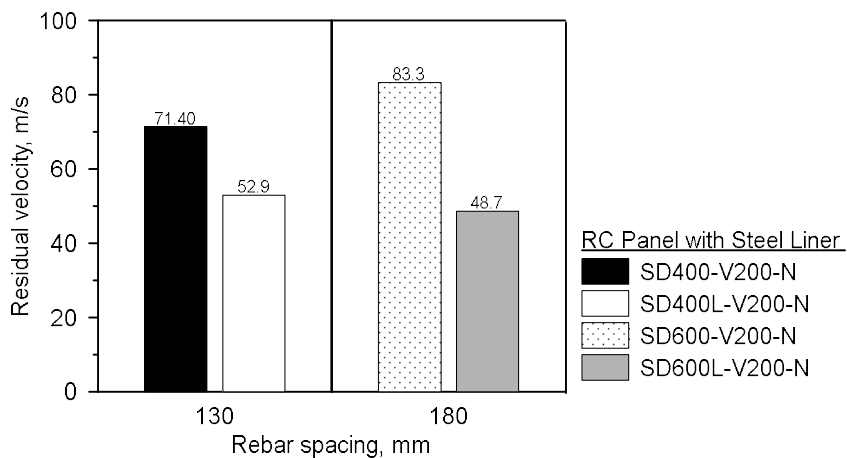
Figure 3.5 Residual velocity of each test specimen at V200
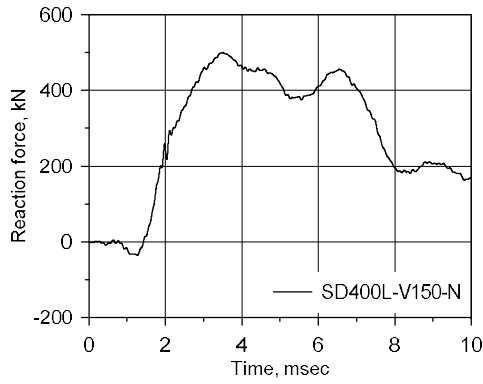
(a) SD400L-V150-N
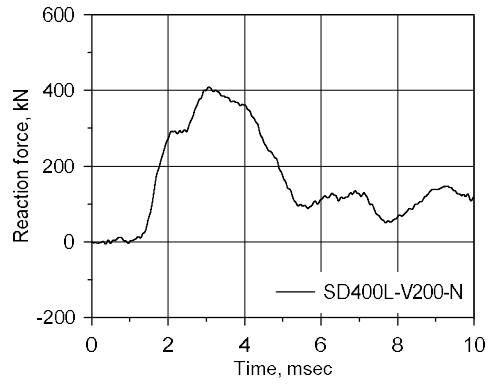
(d) SD400L-V200-N
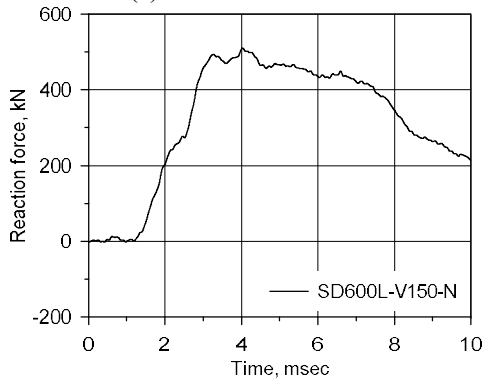
(c) SD600L-V150-N
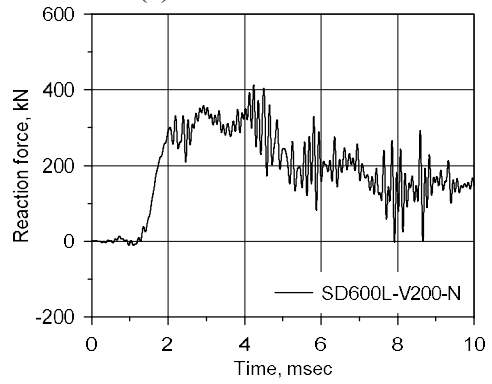
(d) SD600L-V200-N

Figure 3.6 Reaction force time history of RC panels with steel liner

4 4

3.1.3. Effect of rebar collision

The effect of rebar collision was investigated at the impact velocity of 200 m/s. While keeping the same reinforcement ratio of the test specimen, the location of intersection of horizontal and vertical reinforcing steels were shifted so that it could be positioned at the center of the panels. As shown in Figure 3.7, one horizontal rebar was ruptured in SD400-V200-D, and both horizontal and vertical rebars were ruptured in SD600-V200-D from the impact. As a result, the residual velocity of the projectile was remarkably reduced; the one impacted SD400-V200-D rebounded back to the front side of the specimen. According to Zhang et al. (2020), the RC target showed increase resistance against penetration caused by the directed resistance from the impact with steel reinforcement. The test results are summarized in Table 3.5.

(a) SD400-V200-D   (b)SD600-V200-D
Figure 3.7 Front side of RC panels with rebar collision

Table 3.5 Test results of rebar collision cases

Specimen ID	Failure mode	Number of broken rebars	Residual velocity (m/s)
SD400-V200-N	Perforation	-	71.4
SD600-V200-N	Perforation	Front: 1H	Rebound
SD400-V200-D	Perforation	-	83.3
SD600-V200-D	Perforation	Front: 1H, 1V Rear: 1V	Not measured

For the rear side of the test specimens, severe deformation in reinforcing steel that was directly impacted by the projectile was observed. Especially, a vertical reinforcing steel in SD600-V200-D specimen was ruptured as shown in Figure 3.8. For reaction forces measured during the impact test, Figure 3.9 shows the reaction force time history of RC panels with rebar collision. Compared to those of RC panels with no rebar collision, which were around 330 kN, reaction forces with rebar collision were greater. It might be due to the reinforcing steels transferred greater applied forces directly to the supports, showing its peak values earlier than those of no rebar collision cases.
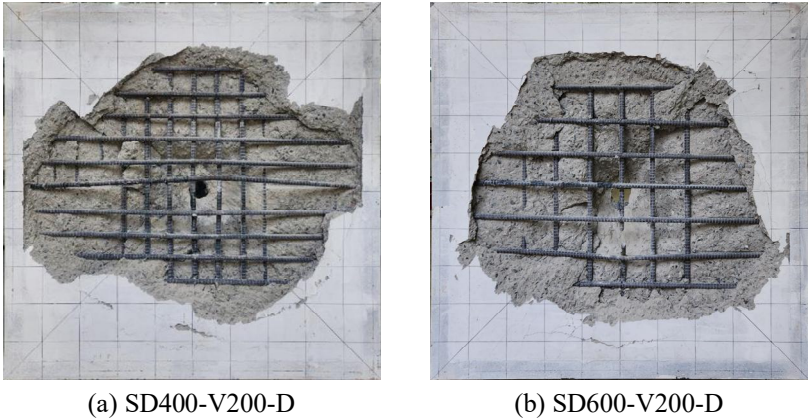
(a) SD400-V200-D   (b) SD600-V200-D
Figure 3.8 Rear side of RC panels with rebar collision
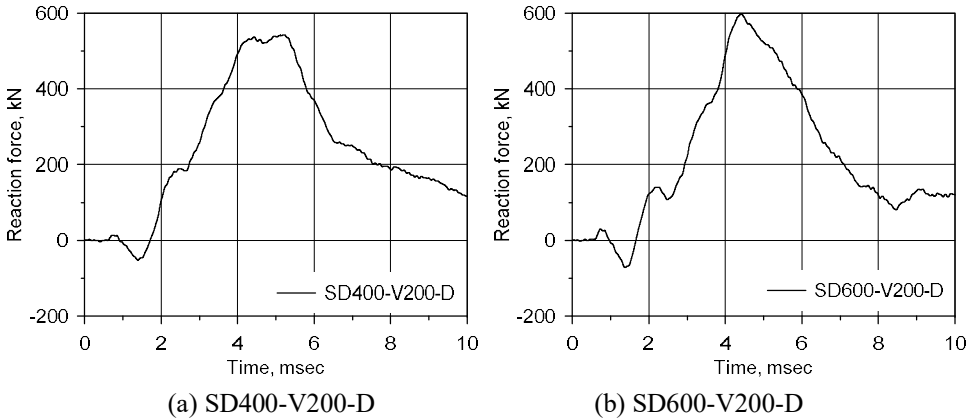
(a) SD400-V200-D   (b) SD600-V200-D
Figure 3.9 Reaction time history for RC panels with rebar collision

3.2. Damage assessment

As mentioned before, the damaged areas on front and rear side of RC panels were calculated by an image processing technique and normalized to the total surface of the panels. To evaluate the effects of rebar spacing, steel liner and rebar collision, all test results were plotted into one chart in the following sections.

3.2.1. Spalling area

In Figure 3.10, spalling area on the front side of RC panels are plotted according to the impact velocity of the projectiles. As rebar spacing increased, RC panels exhibited smaller spalling area at impact velocity of 150 m/s, however, spalling area showed less significant change at impact velocity of 200 m/s. However, the spalling areas exhibited both increasing and decreasing tendency when the rear steel liner was present. In other words, there was no apparent correlation between the spalling area and steel liner. Lastly, the effect of rebar collision on spalling area of RC panels was investigated, and the test results indicated that there was no apparent correlation between the spalling area and rebar collision.
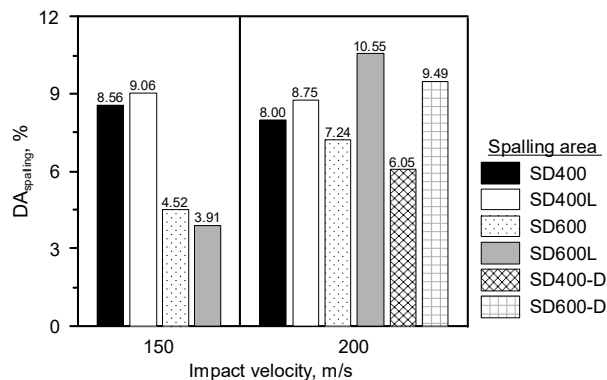
Figure 3.10 Spalling area of test specimens

3.2.2. Scabbing area

For scabbing area on the rear side, RC panels with wider rebar spacing and rebar collision exhibited greater damaged areas. Also, RC panels with rebar collision showed greater scabbing area. This might be of significant deformation of reinforcing steel on the rear side, extending the range in which concrete cover is ejected from the rear side. On the other hand, the rear steel liner prevented the scabbing of RC panels, resulting in no scabbing area as shown in Figure 3.11. Increase in scabbing area could impose greater threats to internal equipment and personnel in case of aircraft collision on NPP structures. Thus, it is crucial to investigate the integrated effect of rebar spacing, steel liner and rebar collision on scabbing area of RC panels.
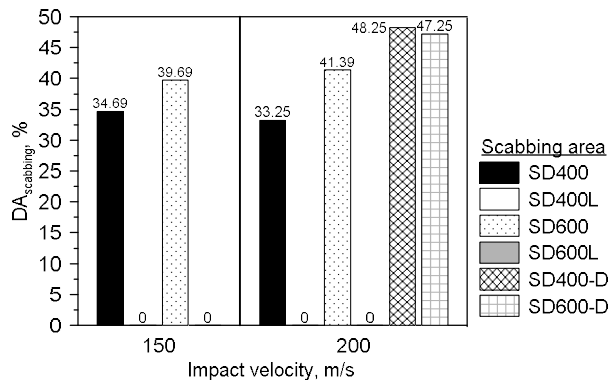
Figure 3.11 Scabbing area of test specimens

4. Modification of empirical formula

In this study, assessment on existing empirical formulas was carried out for prediction of perforation limit of RC panels under hard impact. Based on the assessment, a modification empirical formula was suggested, which was fitted to the test results of this study. To overcome the limitations of existing empirical formulas, which do not consider the effect of reinforcing steel and steel liner, an additional term was introduced to account for the effect of the rebar spacing and diameter of the projectile. The modification process was divided into three different steps as follows.
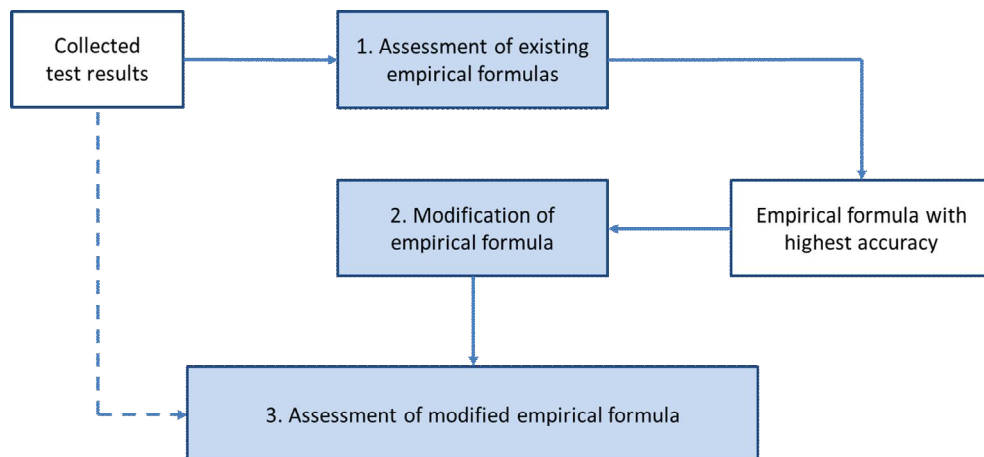
Figure 4.1 Schematic of modification process of empirical formula

Total of 82 impact test cases on RC panel from 10 different studies, including this study, were collected for the assessment of existing empirical formulas. Panel thickness, concrete strength, rebar ratio and projectile's diameter and impact velocities were considered as shown in Table 4.1. With the empirical formula that shows the best prediction of test results, a modification was made so that the modified empirical formula could predict the test result of this study with

consideration of the rebar spacing and diameter of the projectile. Lastly, the modified empirical formula is assessed with the collected test data followed by the discussion.

Table 4.1 Collection of test data from impact test on RC panel hard impact

Tests	Data (EA)	Concrete			Projectile	
		Panel thickness (mm)	Concrete strength (MPa)	Rebar ratio (%)	Diameter (mm)	Impact velocity (mm)
Hanchack et al. (1992)	15	178	48-140	0.16	25.4	301-1058
Dancygier et al. (1996)	6	40-60	34-104	0.41-0.71	25	85-143
Dancygier et al. (2007)	16	200	40-119	0.14-0.42	50	203-292
Alumsallam et al. (2013)	6	90	40.5-59.5	0.71	40	91-125.5
Alumsallam et al. (2015)	3	90	64.5	0.37	40	108.1-135.2
Abdel-Kader et al. (2014)	3	100	26	0.36	40	302-313
Wu et al. (2015)	20	100-200	75-96.5	0.16-0.36	25.3	536-731
Dancygier et al. (2014)	5	200	89.5-112.3	0.21	50	239-281
Lee et al. (2021)	4	500	49.4	0.63-0.87	85	100-200
This study	4	500	49.9	0.63-0.87	85	150-200
Total	82	40-500	26-119	0.14-0.87	25-85	85-1058

4.1 Assessment of existing empirical formulas

4.1.1 Empirical formulas recommended by NPP design codes

Based on the test results of this study, it is inferred that prediction of perforation limit velocity, which is the minimum impact velocity at which RC panel experiences perforation, is more adequate for two reasons. First is that scabbing failure is prevented by the rear steel liner on the RC panels, and the second is that the failure modes observed in the test are mostly perforations. Therefore, empirical formulas suggested by NPP design codes for perforation limits are expressed in terms of perforation limit velocity as shown in Table 4.2. To assess the empirical formulas, test parameters of this study have been used in the following section.

Table 4.2 Perforation limit velocity predicted by existing empirical formulas

Empirical formulas	Perforation limit velocity
Modified NDRC	$V_p = d \left[\dfrac{G d \sqrt{f_c}}{N^* M \left(3.8 \times 10^{\wedge} -5\right)} \right]^{(1/1.8)}$
Degen	$V_p = d \left[\dfrac{G \cdot d \cdot \sqrt{f_c}}{\left(3.8 \times 10^{-5}\right) N^* M} \right]^{(1/1.8)}$
Chang	$V_p = \dfrac{H}{u^{0.25}} \left(\dfrac{d \cdot f_c}{M} \right)^{0.5}$
Criepi	$V_p = \left[\dfrac{H}{0.9 u^{0.25}} \left(\dfrac{d \cdot f_c}{M} \right)^{0.5} \right]^{(1/0.75)}$
CEA-EDF (1974)	$V_p = 1.3 \rho^{1/6} f_c^{0.5} \left(\dfrac{P H^2}{\pi M} \right)^{2/3}$

Since the empirical formulas listed in Table 4.2 do not consider the effect of reinforcement, they predict the constant perforation limit velocity regardless of

rebar spacing as shown in Figure 4.2. This indicates that current empirical formulas not only overestimate the impact resistance of the RC panels, but also failed to account for the decrease in its resistance as rebar spacing increased. To specify, all RC panels at impact velocity of 200 m/s showed perforation failure when empirical formulas predicted non-perforation mode at given velocity. Furthermore, the RC panels impacted with initial velocity of 150 m/s showed different failure modes depending on the spacing of reinforcing steels.
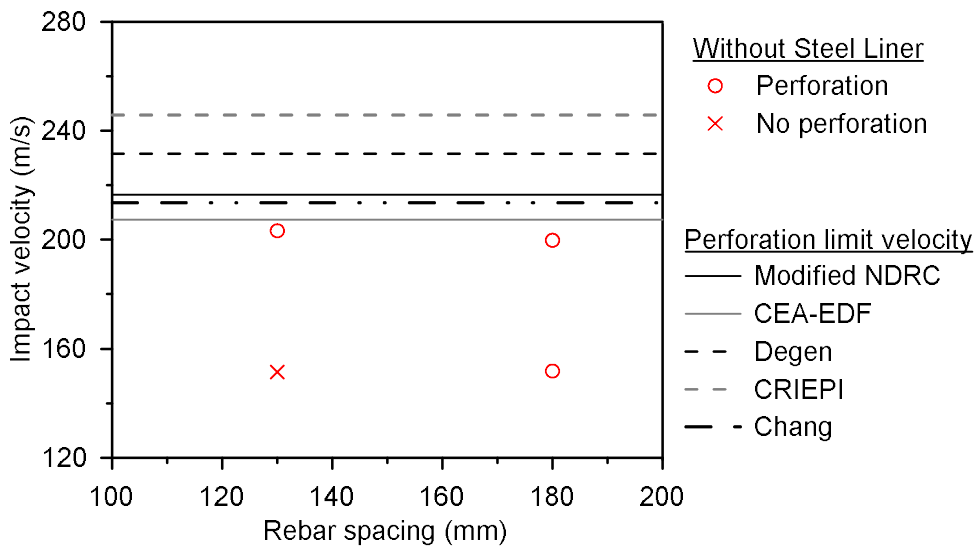
Figure 4.2 Predicted perforation limit velocity by empirical formulas

Although details of test specimen used in the suggestion of empirical formulas were limited, there was evidence that explained the overestimation of the impact resistance of RC panels. Figure 4.3 shows the rear side of RC panel used in the suggestion of CEA-EDF formula in 1974. It can be clearly seen that the diameter of projectile was larger than the spacing of reinforcing steels, which provides direct resistance to the progression of projectile into the concrete target. However, the impact condition considered in this study for evaluation of impact resistance of RC

panels assumed no direct collision with rebars, which is considered more critical condition. Furthermore, Kennedy (1976) mentioned that the ratio of panel thickness to diameter of projectile in impact tests were substantially less than 3, where the ratio in this study was 5.88.

Figure 4.3 Perforation of RC panel (Berriaud (1978))

4.1.2 Empirical formulas with consideration of reinforcement

There are three empirical formulas that consider the effect of reinforcement as shown in Table 4.3. For UMIST formula, which do not consider the effect of reinforcement for case with ratio of panel thickness to projectile's diameter is greater than 5, CEA-EDF and UKAEA formulas predicted that the perforation limit velocity would decrease as the rebar spacing increases. However, SD600-V150-N specimen which has rebar spacing of 180mm and impact velocity of 150m/s failed in perforation without total perforation of the RC panel. But empirical formulas overestimated the impact resistance of SD600-V150-N with huge discrepancies. Thus, a modification is needed based perforation limit case shown in SD600-V150-N.

Table 4.3 Empirical formulas with consideration of reinforcement

Empirical formulas	Perforation limit velocity
CEA-EDF (1991)	$$V_p = 1.3 \rho_c^{1/6} f_c^{1/2} \left(\frac{pH^2}{\pi M} \right)(r+0.3)^{1/2}$$
UKAEA	$$V_p = \begin{cases} V_a & \text{for } V_p \geq 70 \text{ m/s} \\ V_a\left[1+\left(\frac{V_a}{500}\right)^2\right] & \text{for } V_p < 70 \text{ m/s} \end{cases}$$ where, $V_a = 1.3 \rho_c^{1/6} f_c^{1/2} \left(\frac{pH^2}{\pi M} \right)(r+0.3)^{1/2}\left[1.2-0.6\left(\frac{c_r}{H}\right)\right]$
UMIST	$$V_p = \sqrt{2E_p / M}$$ $$E_p = \begin{cases} \eta \sigma_t d^3 \left[-0.01\left(\frac{H}{d}\right)+0.02\left(\frac{H}{d}\right)^3 \right] & \text{for } 1 \leq \frac{H}{d} < 5 \\ \sigma_t d^3 \left(\frac{\pi}{4}\left[\left(\frac{H}{d}-3.0\right)\right]\right) & \text{for } \frac{H}{d} \geq 5.0 \end{cases}$$ where, $\eta = \begin{cases} \frac{3}{8}\left(\frac{d}{c_r}\right)r_t + 0.5 & \text{for } \left(\frac{d}{c_r} < \sqrt{\left(\frac{d}{d_r}\right)}\right) \\ \frac{3}{8}\left(\sqrt{\left(\frac{d}{d_r}\right)}\right)r_t + 0.5 & \text{for } \left(\frac{d}{c_r} \geq \sqrt{\left(\frac{d}{d_r}\right)}\right) \end{cases}$
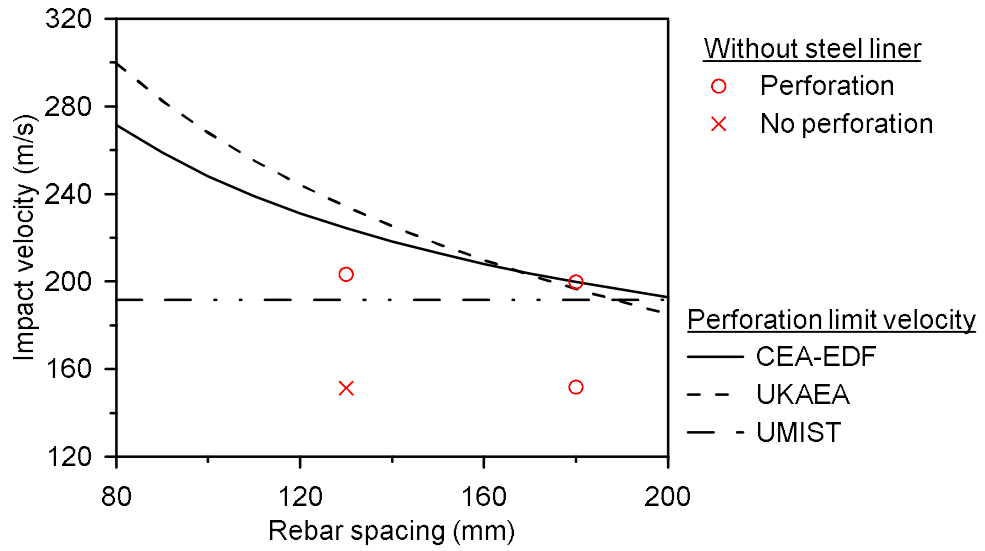
Figure 4.4 Perforation limit velocity with reinforcement consideration

4.1.3 Assessment of empirical formulas

To select the empirical formula for the modification, collected test results were categorized into two modes: perforation or non-perforation. Then, the accuracy of each aforementioned empirical formula has been evaluated as shown in Table 4.4.

Table 4.4 Accuracy of existing empirical formulas

Tests	Data (EA)	Accuracy					
		CEA-EDF	Modified NDRC	UKAEA	Degen	Criepi	Chang
Hanchack et al. (1992)	15	0.87	0.93	0.60	0.87	0.47	0.53
Dancygier et al. (1996)	6	0.67	0.50	0.67	0.50	0.67	0.67
Dancygier et al. (2007)	16	0.38	0.38	0.38	0.38	0.38	0.38
Alumsallam et al. (2013)	6	0.50	0.50	0.50	0.50	0.50	0.50
Alumsallam et al. (2015)	3	0.67	0.67	0.67	0.67	0.67	0.67
Abdel-Kader et al. (2014)	3	0.00	0.00	0.00	0.00	0.00	0.00
Wu et al. (2015)	20	1.00	1.00	0.90	0.80	0.80	0.95
Dancygier et al. (2014)	5	0.00	0.00	0.00	0.00	0.00	0.00
Lee et al. (2021)	4	0.50	0.50	0.50	0.50	0.50	0.50
This study	4	0.50	0.25	0.25	0.25	0.25	0.25
Total	82	0.63	0.62	0.55	0.61	0.50	0.55

Based on the results, CEA-EDF and modified NDRC showed the best prediction. In case of CEA-EDF, it considers the effect of reinforcement, so it was chosen for the modification in the following section.

4.2. Modification of empirical formula

4.2.1. Proposed modification of empirical formula

Eq. 4.1 shows the modified empirical formula to account for the effect of rebar spacing. Here, parameters representing the diameter of projectile and rebar spacing were added since existing empirical formulas, especially CEA-EDF, had been proposed based on the test results that included the influence of rebar collision, resulting in overestimation of the impact resistance of RC panels. Then, the coefficient was determined so that the perforation limit case, SD600-V150-N, would lie on the predicted perforation limit velocity line as shown in Figure 4.5

$$V_p = 1.3\rho_c^{1/6} f_c^{1/2} \left(\frac{pH^2}{\pi M} \right) (r+0.3)^{1/2} \left(\frac{d_p}{c_r} \right)^{0.317} \qquad \text{Eq. (4.1)}$$
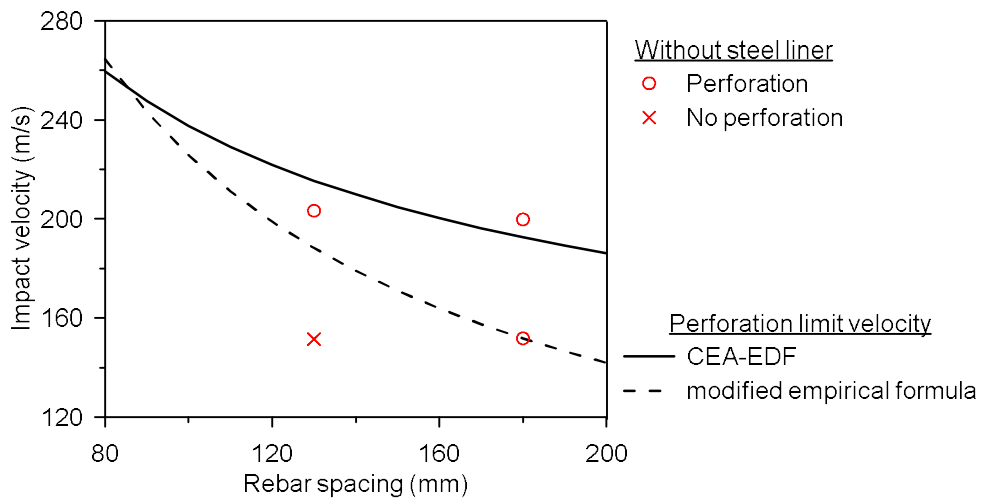
Figure 4.5 Perforation limit velocity by modified empirical formula

4.2.2. Applicable range of the modified empirical formula

The addition of the ratio of the diameter of projectile to rebar spacing allows accounting for not only the impact condition, but also the effect of the relative size of the test specimen and projectile. Since the test results used for the modification is limited to impact condition which did not collide with the reinforcing steel, the proposed formula assumes the diameter of the projectile is smaller than the rebar spacing. Thus, in cases where the projectile is expected to be colliding with reinforcing steel, the original CEA-EDF should be used to predict the perforation limit velocity.

4.3. Assessment of modified empirical formula

4.3.1. Model verification

Total of 82 previously collected from 10 different studies including this study were used to verify the modified empirical formula. As it can be seen in Table 4.5 below, the modified empirical formula showed the best prediction of test results owing to predicting test results from Lee et al. (2021) and this study. It is to be noted that the modification was made to the original CEA-EDF formula with a single data from this study. Therefore, parametric study is to be made for suggestion of more robust and reliable predictive formula in future study through numerical simulation or additional experiments.

Table 4.5 Accuracy of modified empirical formula

Tests	Data (EA)	Accuracy						
		Existing empirical formula						Modified empirical formula
		CEA-EDF	Modified NDRC	UKAEA	Degen	Criepi	Chang	
Hanchack et al. (1992)	15	0.87	0.93	0.60	0.87	0.47	0.53	0.80
Dancygier et al. (1996)	6	0.67	0.50	0.67	0.50	0.67	0.67	0.50
Dancygier et al. (2007)	16	0.38	0.38	0.38	0.38	0.38	0.38	0.50
Alumsallam et al. (2013)	6	0.50	0.50	0.50	0.50	0.50	0.50	0.67
Alumsallam et al. (2015)	3	0.67	0.67	0.67	0.67	0.67	0.67	1.00
Abdel-Kader et al. (2014)	3	0.00	0.00	0.00	0.00	0.00	0.00	1.00
Wu et al. (2015)	20	1.00	1.00	0.90	0.80	0.80	0.95	1.00
Dancygier et al. (2014)	5	0.00	0.00	0.00	0.00	0.00	0.00	0.00
Lee et al. (2021)	4	0.50	0.50	0.50	0.50	0.50	0.50	1.00
This study	4	0.50	0.25	0.25	0.25	0.25	0.25	1.00
Total	82	0.63	0.62	0.55	0.61	0.50	0.55	0.74

4.3.2. Prediction of RC panels with steel liner

For evaluation of the impact resistance of RC panels with steel liner, an equivalent concrete thickness equation was used. Tsubota et al. (1993) suggested that the rear steel liner could be converted to equivalent concrete thickness as shown in Figure 4.6.
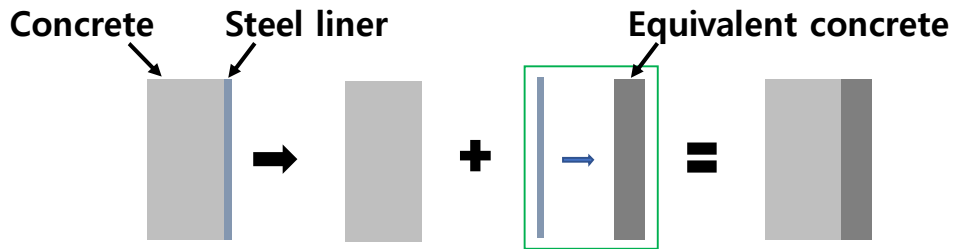
Figure 4.6 Equivalent concrete thickness of rear steel liner

Eq 4.2 shows the equivalent concrete thickness equation for perforation mode. Thus, 2.3 mm thickness steel liner could be converted to 41.9 mm thickness concrete, leaving a new RC panel with thickness of 541.9 mm. Then, CEA-EDF and modified empirical formula are used to predict the perforation limit velocity of the reinforced concrete panels in this study as shown in Figure 4.7.
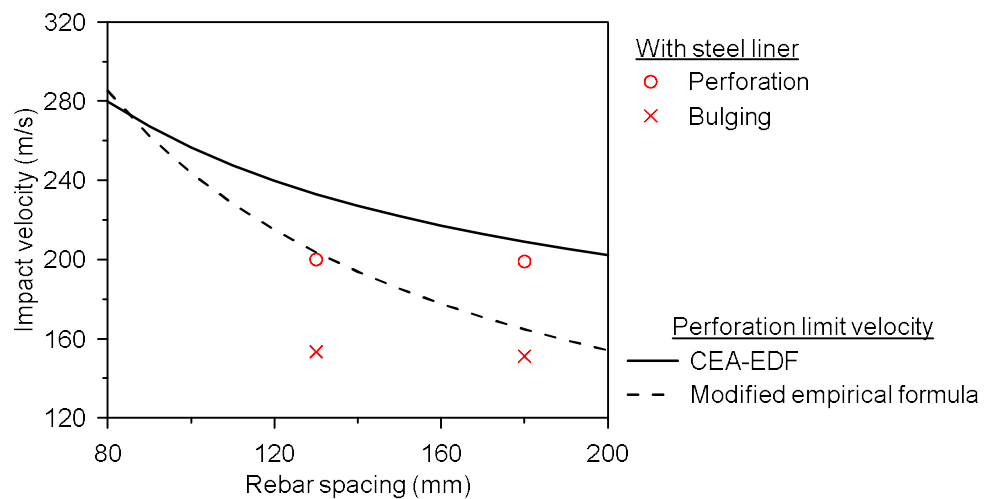
Figure 4.7 Perforation limit velocity of RC panel with steel liner

Perforation limit velocity predicted by both CEA-EDF and modified empirical formulas seemed to overestimate the impact resistance of RC panels with rear steel liner. It is due to the limited applicability of the equivalent concrete thickness equation suggested by Tsubota et al. (1993). However, the modified empirical formula still showed higher predictive accuracy compared to the original CEA-EDF. Therefore, regardless of rear steel liner, modified empirical formula showed better prediction of perforation limit velocity of the RC panels under hard impact.

4.4 Future study

4.4.1. Boundary conditions

In this study, test specimens were fixed on both side by four edge supports. However, other previous studies have employed different boundary condition as shown in Table 4.6. Given the local damages under impact loading takes place within the supports, it might be of insignificant effect coming from the boundary condition. However, it is author's intention to study the effects of boundary condition on impact behavior of RC panels in various test settings.

Table 4.6 Support conditions of impact tests

Reference	Support condition
Lee et al. (2021)	Four-edge support
Abdel-Kader et al. (2015)	Two-edge support
Riedel et al. (2010)	Four-point support
Tai (2009)	Edge support
Dancygier and Yankelevsky (1996)	Four-point support
Sugano et al. (1993)	Four-point support
Ohno et al. (1992)	Suspended
Kojima (1991)	Four-point support
Stephenson et al. (1978)	Four-edge support
This study	Four-edge support

4.4.2. Standardization of projectile

For the evaluation of local behavior of structures, DOE-STD-3014-2006 considers relatively rigid components of aircraft such as landing gear and engine shaft as missile. Although a renowned empirical formula, modified NDRC, takes account of nose shape of the projectile in assessment of local behavior of RC panels under hard impact, there is no standardized method for fabrication or determination of the projectile's shape, mass or material for consistent evaluation of structure's impact resistance. Therefore, it is author's another intention to investigate on the effect of properties of the projectile in simulated aircraft impact tests, and to suggest predictive model for local failure of structures.

5. Conclusion

In this study, special design considerations of nuclear power plant (NPP) structures were discussed, and an assessment of the current status of NPP design codes was conducted. It was found that the empirical formulas recommended by design codes do not consider the effects of reinforcing steel and steel liner. Thus, an experimental study was performed to investigate the effects of reinforcing steel and steel liner on impact resistance of RC panels with yield strength, steel liner, impact velocity and condition as main variables. A total of 10 RC panels scaled with 1:2.4 similarity ratio to APR1400 were prepared for simulated aircraft collision on NPP structures.

The effects of rebar spacing, steel liner and impact condition were investigated through series of impact tests. The impact resistance of RC panels were evaluated in terms of perforation resistance, damage assessment of RC panels. It was found that wider rebar spacing exhibited lower perforation resistance owing to more critical failure mode with greater residual velocity of the projectile, and greater damaged area were induced on both front and rear face of the panel under the same applied impact force by hard projectile.

However, the presence of steel liner embedded on the rear side of RC panels showed remarkable enhancement on impact resistance of RC panels. The rear steel liner not only prevented the scabbing failure by trapping the concrete fragment bursting off the rear side, but it also reduced the residual velocity of the projectile for both panels with different rebar spacing. In other words, when steel liner was reinforced on the rear side of the RC panel, the effect of rebar spacing which was reduced.

In case of rebar collision, the RC panels with direct rebar collision showed remarkable enhancement in perforation resistance. To specify, projectiles that

collided with reinforcing steel showed very low or no residual velocity due to the direct resistance from rebars. However, the scabbing areas observed on the rear side of the panels were much greater than those of RC panels without direct rebar collision.

Based on test results, a modified empirical formula was proposed by modifying the previous empirical formula that showed the better prediction of test results from previous impact tests. As a result, existing and the proposed empirical formula were compared and analyzed through previous research data, confirming that the modified empirical formula showed better prediction than others. Furthermore, the perforation limit velocity for RC panels with rear steel liner was predicted by converting the steel liner into an equivalent concrete thickness. It was shown that the proposed empirical formula showed better predictive accuracy regardless of the steel liner. However, there was only 1 test case in which perforation limit was observed, which means more test data are required for further verification of the modified empirical formula. Therefore, it is necessary to conduct numerical study to obtain more test data for suggestion of better predictive model for RC panels under impact loading.

Lastly, discussions on effects of boundary conditions and properties of the projectile are made. Although all the local failure of RC panels took place within the boundaries of the test setup, different support conditions among numerous researchers infer that there needs to be a standardized method for consistent evaluation of the impact resistance of RC panels under impact loadings.

Reference

Abdel-Kader, M., and A. Fouda. Effect of reinforcement on the response of concrete panels to impact of hard projectiles. International Journal of Impact Engineering 2014;63;1-17.

Abbas, H., N. Siddiqui., T. Almusallam., A. Abadel., H. Elsanadedy., and Y. Al-Salloum. Effect of rebar spacing on the behavior of concrete slabs under projectile. Structural Engineering and Mechanics 2021;77;3;329-342.

ACI Committee 349, Code Requirements for Nuclear Safety-Related Concrete Structures (AC 349-13) & Commentary, American Concrete Institute, Farmington Hills, MI, 2014.

ACI Committee 370, "Report for the Design of Concrete Structures for Blast Effects", Farmington Hills, MI, American Concrete Institute, 2014.

Alumusallm, T.H., A.A. Abadel, Y.A. Al-Salluom., N.A. Siddiqui., H. Abbas. Effectiveness of hybrid-fibers in improving the impact resistance of RC slabs. International Journal of Impact Engineering 2015;81-1;61-73.

Almusallam, T.H., N.A. Siddiqui., R.A. Iqbal., H. Abbas. Response of hybrid-fiber reinforced concrete slabs to hard projectile impact. International Journal of Impact Engineering 2013;58-1;17-30.

ASTM C39/C39M-20b. Standard Test Method for Compressive Strength of Cylindrical Concrete Specimens, ASTM International, West Conshohocken, PA, 2020.

Berriaud, C., A. Sokolovsky, R. Gueraud, J. Dulac, R. Labrot. Local behaviour of reinforced concrete walls under missile impact. Nuclear Engineering and Design 1978;45;457-469.

Dancygier, A.N., D.Z. Yankelevsky. High strength concrete response to hard projectile impact. International Journal of Impact Engineering 1996;18-6;583-599.

Dancygier A.N., D.Z. Yankelevsky. Effects of Reinforced Concrete Properties on Resistance to Hard Projectile Impact. ACI Structural Journal 1999;96(2);259-267.

Dancygier, AN., DZ. Yankelevsky., and C. Jaegermann. Response of high performance concrete plates to impact of non-deforming projectiles. International Journal of Impact Engineering 2007;34;1768-1779.

Dancygier A.N., A. Katz., D. Benamou., D.Z. Yankelevsky. Resistance of double-layer reinforced HPC barriers to projectile impact. International Journal of Impact Engineering 2014;67-1;237-245.

Erin Engineering & Research, Inc. Methodology for performing aircraft impact assessments for new plant designs. Erin Engineering & Research, Inc. California. 2009.

Fang, Q. and H. Wu, "Concrete Structures Under Projectile Impact, in Concrete Structures Under Projectile Impact", Springer, pp. 497-558, 2017.

Galan, M., and N. Orbovic. Quantification of perforation resistance of prestressed walls with transverse reinforcement and liner under hard missile impacted on test results. Proceedings SMiRT 23 2015;Div V;554.

Goli, H.B., Gesund H. Yield Line Analysis of Orthotropically Reinforced Exterior Panels of Flat Slab Floors. Advances in Concrete Slab Techonology 1980;149-159.

Hanchak, S.J., M.J. Forrestal., E.R. Young., and J.Q. Ehrgott. Perforation of concrete slabs with 48 MPa (7ksi) and 140 MPa (20ksi) Unconfined compressive strengths. International Journal of Impact Engineering 1992; 12(1); 1-7.

Hashimoto, J., K. Takiguchi., K. Nishimura., M. Tsutusi., Y. Ohashi., and H. Torita. Experimental study on behavior of RC panels covered with steel plates subjected to missile impact. Proceddings SMiRT 18 2005;J05;4.

Huang, F., H. Wu., Q. Jin., and Q. Zhang. A numerical simulation on the perforation of reinforced concrete targets. International Journal of Impact Engineering 2005;32;173-187.

Kennedy R.P. A review of procedures for the analysis and design of concrete structures to resist missile impact effects. Nuclear Engineering and Design 1976;37;183-203.

Kojima I. An experimental study on local behavior of reinforced concrete slabs to missile impact. Nuclear Engineering and Design 1991;130;121-132.

Lee, S., C. Kim., Y. Yu., and J.-Y. Cho. Effect of reinforcing steel on the impact resistance of reinforced concrete panel subjected to hard-projectile impact. International Journal of Impact Engineering 2021;148;103762.

Li, Q.M., S.R. Reid, H.M. Wen, and A.R. Telford, "Local impact effects of hard missiles on concrete targets", International Journal of Impact Engineering, 2005, 32, pp. 224-284.

Ohno, T., T. Uchida, N. Matsumoto, Y. Takahashi. Local damage of reinforced concrete slabs by impact of deformable projectiles. Nuclear Engineering and Design 1992;138(1);45-52.

Reidel W., M. Nöldgen, E. Straßburger, K. Thoma, E. Fehling. Local damage to Ultra High Performance Concrete structures caused by an impact of aircraft engine missiles. Nuclear Engineering and Design 2010;240(10);2633-2642.

Stephenson A.E., G.E. Sliter, E.G. Brudette. Full-scale tornado-missile impact tests. Nuclear Engineering and Design 1978;46(1);123-143.

Sugano, T., H. Tsubota, Y. Kasai, N. Kohika, H. Ohnuma, W.A. Riesemann, D.C. Bikel, M.B. Parks. Local damage to reinforced concrete structures caused by impact of aircraft engine missiles Part 1. Test program, method and results. Nuclear Engineering and Design 1993;140(3);387-405.

Tai Y.S. Flat ended projectile penetrating ultra-high strength concrete plate target. Theoretical and Applied Fracture Mechanics 2009;51(2);117-128.

Tsubota, H., Y. Kasai., N. Koshika., H. Morikawa., T. Uchida., T. Ohno., and K. Kogure. Quantitative studies on impact resistance of reinforced concrete panels with steel liners under impact loading part 1: scaled model impact tests. SMiRT 12 1993.

U.S. Department of Energy. Accident analysis for aircraft crash into hazardous facilities. Washington D.C., U.S: Department of Energy Standard DOE-STD-3014-2006; 2006.

Wu, H., Q. Fang, Y. Peng, Z.M. Gong, and X.Z. Kong. Hard projectile perforation on the monolithic and segmented RC panels with a rear steel liner. International Journal of Impact Engineering 2015; 76; 232-250.

국문초록

충격 하중을 받은 **RC** 벽체의 내충격 성능에 철근과 강재 라이너가 미치는 영향에 대한 실험적 연구

예 준 휘

원자력 구조물(NPP)의 설계는 지진, 쓰나미와 테러 공격과 같은 극한상황에 대한 안전을 보장하기 위해 보수적인 설계를 수행하게 된다. 따라서 일반적인 사회기반시설에서 요구되는 것 외에도 철근의 항복강도 제한, 강재 라이너(CLP)의 설계 및 내충격 설계 등을 고려해야하는 특별한 설계 고려사항들이 존재한다. 특히, 철근의 항복강도 제한은 원전 구조물의 효율적인 설계를 저해하고 있으며, 이로 인해 높은 시공비용과 철근혼잡에 의한 콘크리트 품질 저하를 초래하고 있다. 이에 고강도 철근의 적용을 통한 철근량을 줄이기 위한 다양한 연구가 진행되고 있다. CLP 의 경우 방사선 차폐역할을 위해 두꺼운 콘크리트 벽체 내부에 설치하는 동시에, 시공단계에서부터 영구 거푸집으로 배치된다. 마지막으로, 미국 원자력규제위원회는 새로 설계된 원자력 발전소에 대해 최근 대형 항공기 충돌이 미치는 영향을 평가하도록 규정 개정을 발표하였다.

항공기 충돌에 대한 NPP 구조물의 내충격 설계를 위해 ACI 349-13, DOE-STD-3014-2006 및 NEI 07-13 과 같은 NPP 관련 설계기준에서는

RC 벽체에 내한 충돌실험을 기반으로 제안된 다양한 국부손상 예측 경험식을 추천하고 있다. 하지만 경험식에서 고려하는 변수는 콘크리트 벽체와 발사체의 특성에 한정적이라는 한계점이 존재한다. 즉, NPP 구조물의 내충격 설계에 앞서 언급된 철근 및 강재 라이너의 영향을 하지 않으므로 효율적인 설계를 위해서는 RC 벽체의 내충격 성능에 미치는 철근과 강재 라이너의 영향에 대한 조사가 필요하다.

선행연구조사를 통해 철근 및 강재 라이너가 RC 벽체의 내충격 성능에 철근 간격, 충돌 조건 및 강재 라이너가 큰 영향을 미치는 것을 확인했다. 그러나 선행연구에서는 NPP 구조물의 내충격 성능에 미치는 철근과 강재 라이너가 미치는 영향을 분석에 제한적이었으며, 이는 대부분의 선행연구에서는 벽체의 설계강도가 변했기 때문에 순수한 철근에 의한 영향을 분석하지 못한다는 점이다. 또한, 강재 라이너의 영향을 조사한 선행연구에서는 RC 벽체 내 철근을 고정변수로 설정하여 철근과 강재 라이너간의 상관관계에 대한 분석이 제한적이다는 한계점이 있었다. 따라서, 본 논문에서는 철근 간격, 충돌 조건 및 강재 라이너 유무가 RC 벽체의 내충격 성능에 미치는 영향 및 매커니즘 조사를 연구 목적으로 설정하였으며, 이를 위해 총 10 개의 시험체에 대해 항공기 충돌 모사 실험을 수행하였다.

철근의 항복강도, 강재 라이너의 유무, 충돌 속도 및 발사체 충돌 조건을 주요 변수로 설정하였다. RC 벽체와 강재 라이너의 설계는 한국의 원전 구조물인 APR1400 을 1:2.4 상사비를 적용하여 설계하였다. 또한, 발사체의 경우 NPP 관련 설계기준에서 제안하고 있는 항공기의 엔진 쉐프트를 동일한 상사비를 적용하여 설계하였다. RC 벽체의 내충격 성능은 관통저항성능과 국부손상정도를 통해 평가하였으며, RC 벽체의 파괴모드, 발사체의 잔류속도, 반력 그리고 벽체 전후면에 발생한

파괴면적을 통해 각 변수가 RC 벽체의 내충격 성능에 미치는 영향을 평가하였다. 그 결과, 철근 간격이 넓어질수록 벽체의 내충격 성능은 감소하였으며, 강재 라이너로 인한 RC 벽체의 내충격 성능은 크게 증진되는 것을 확인하였다. 하지만, 발사체가 철근을 충돌한 경우에는 RC 벽체의 관통저항성능은 크게 증진되었으나, 배면부에 발생한 파괴면적은 크게 증가하는 경향을 확인하였다.

마지막으로 기존의 경험식 중 하나를 기반으로 철근 간격과 발사체 직경의 영향을 고려할 수 있는 수정식을 제안하였다. 제안된 수정식은 선행연구 및 본 논문의 실험 결과를 통해 평가하였으며, 수정식이 본 논문뿐만 아니라 선행 연구의 관통한계속도를 가장 잘 예측하는 것을 확인하였다. 그러나 본 논문의 경우, 하나의 데이터를 기반으로 수정이 수행되었기 때문에 본 논문의 실험범위 밖의 상황에 대한 적용성에 대한 한계점이 존재할 것으로 판단된다. 따라서 추후 RC 벽체의 내충격 성능에 대한 신뢰성 있는 예측을 위해 수치적 및 매개변수 해석을 통한 추가적인 데이터를 활용하여 수정식을 제안하고자 한다.

주요어: 내충격 성능, 항공기 충돌실험, 강재 라이너, 국부손상 예측 경험식, 고강도 철근, 원전 구조물